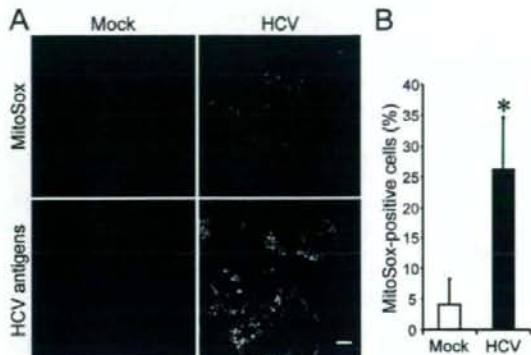FIG. 6. HCV infection induces cytochrome *c* release and caspase 9 activation in Huh7.5 cells. (A) Cytochrome *c* release. Mitochondrial and cytosolic fractions were prepared from HCV-infected cells and the mock-infected control at 6 days postinfection and analyzed by immunoblotting using antibodies against cytochrome *c*, Tim23, NS3, and actin. Can Get Signal (Toyobo, Osaka, Japan) was used to obtain stronger signals for cytochrome *c*. Amounts of Tim23 and actin were measured to verify equal amounts of mitochondrial and cytosolic fractions, respectively. Also, Tim23 was used to show successful separation of mitochondria. (B) Caspase 9 activation. Caspase 9 activities in cells infected with HCV and mock-infected controls were measured at 0, 2, 4, and 6 days postinfection. The caspase 9 activity of the control cells at day 0 postinfection was arbitrarily expressed as 1.0. Data represent means ± standard deviations (SD) of three independent experiments. *, $P < 0.05$, compared with the control. (C) HCV infection induces a marginal degree of caspase 8 activation. Caspase 8 activities in cells infected with HCV and mock-infected controls were measured at 0, 2, 4, and 6 days postinfection. The caspase 8 activity of the control cells at day 0 postinfection was arbitrarily expressed as 1.0. Data represent means ± SD of three independent experiments. *, $P < 0.05$, compared with the control.

FIG. 7. HCV infection induces increased production of mitochondrial superoxide in Huh7.5 cells. (A) Mitochondrial superoxide production in HCV-infected cells and the mock-infected control was examined at 6 days postinfection. Cells were directly incubated with MitoSOX (upper row) and then stained for HCV antigens by using an HCV-infected patient's serum, followed by FITC-labeled goat anti-human IgG (bottom row). Scale bar, 10 μm. (B) Quantification of MitoSOX-stained cells. The percentages of cells stained with MitoSOX were determined for HCV-infected cultures and the mock-infected control. Data represent means ± standard deviations of three independent experiments. *, $P < 0.05$, compared with the control.

such as the accumulation of unfolded or misfolded proteins in the lumen. On the other hand, in response to ER stress, the unfolded protein response (UPR) is activated to alleviate the ER stress by stimulating protein folding and degradation in the ER as well as by inhibiting protein synthesis (7). The UPR of the host cell is disadvantageous for progeny virus production and may therefore be considered an antiviral host cell response. It was reported that, to counteract the disadvantageous UPR so as to maintain viral protein synthesis, HCV RNA replication suppressed the IRE1-XBP1 pathway, which is responsible for protein degradation upon UPR (59). Also, HCV E2 was shown to inhibit the double-stranded RNA-activated protein kinase-like ER-resident kinase (PERK), which attenuates protein synthesis during ER stress by phosphorylating the alpha subunit of eukaryotic translation initiation factor 2 (45). It is reasonable, therefore, to assume that HCV-infected cells may not necessarily exhibit typical responses to ER stress. In fact, our results revealed that HCV infection in Huh7.5 cells did not enhance
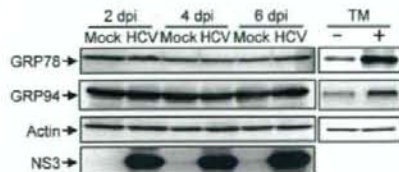
cleavage product truncated Bid (tBid), which facilitates the activation of Bax (63, 68). Under our experimental conditions, however, tBid was barely detected in HCV-infected cells even at 6 days postinfection (data not shown). It is thus likely that caspase 8 activation is marginal and is not the primary cause of Bax activation in our experimental system.

HCV protein expression and HCV RNA replication take place primarily in the ER or an ER-like membranous structure (39, 46). Like other members of the family *Flaviviridae*, such as dengue virus (69), Japanese encephalitis virus (69), West Nile virus (41), and bovine viral diarrhea virus (26), HCV has been reported to induce ER stress in the host cells (5, 14, 17, 55, 60). ER stress is triggered by perturbations in normal ER function,

FIG. 8. HCV infection does not induce ER stress in Huh7.5 cells. Huh7.5 cells infected with HCV and mock-infected controls were harvested at 2, 4, and 6 days postinfection (dpi), and the whole-cell lysates were subjected to immunoblot analysis using antibodies against GRP78, GRP94, NS3, and actin. Amounts of actin were measured to verify equal amounts of sample loading. Huh7.5 cells treated with tunicamycin (TM; 5 μg/ml) for 48 h served as a positive control.

expression of GRP78 and GRP94, which are ER stress-induced chaperone proteins (Fig. 8). Our result thus implies the possibility that ER stress is not crucially involved in HCV-induced apoptosis in Huh7.5 cells. Taking advantage of this phenomenon, we could demonstrate that an ER stress-independent, mitochondrion-mediated pathway plays an important role in HCV-induced apoptosis. In this connection, Korenaga et al. (30) reported that HCV core protein increased ROS production in isolated mitochondria, independently of ER stress, by selectively inhibiting electron transport complex I activity.

In this study, we observed that increased ROS production, Bax activation, and caspase 3 activation were detectable in approximately 15% to 25% of HCV antigen-positive Huh7.5 cells at 6 days postinfection (Fig. 7B, 3D, and 2D, respectively). On the other hand, >90% of the cells in the cultures were confirmed positive for HCV antigens (Fig. 1B). These results imply the possibility that HCV establishes persistent infection in Huh7.5 cells, with a minor fraction of virus-infected cells beginning to undergo apoptosis after a prolonged period of time. Alternatively, it is possible that Huh7.5 cells, though being derived from a cell line (6), are a mixture of two sublineages, with one sublineage being apoptosis prone and the other apoptosis resistant. To test the latter possibility, further cloning of Huh7.5 cells is now under way in our laboratory.

In conclusion, our present results collectively suggest that HCV infection induces apoptosis through a Bax-triggered, mitochondrion-mediated, caspase 3-dependent pathway.

ACKNOWLEDGMENTS

REFERENCES

1. Bantel, H., A. Lügering, C. Poremba, N. Lügering, J. Held, W. Domschke, and K. Schulze-Osthoff. 2001. Caspase activation correlates with the degree of inflammatory liver injury in chronic hepatitis C virus infection. Hepatology 34:758–767.
2. Bantel, H., and K. Schulze-Osthoff. 2003. Apoptosis in hepatitis C virus infection. Cell Death Differ. 10:S48–S58.
3. Barbaro, G., G. Di Lorenzo, A. Asti, M. Ribersani, G. Belloni, B. Grisorio, G. Filice, and G. Barbarini. 1999. Hepatocellular mitochondrial alterations in patients with chronic hepatitis C: ultrastructural and biochemical findings. Am. J. Gastroenterol. 94:2198–2205.
4. Bartenschlager, R., M. Frese, and T. Pietschmann. 2004. Novel insights into hepatitis C virus replication and persistence. Adv. Virus Res. 63:171–180.
5. Benali-Furet, N. L., M. Chami, L. Houel, F. De Giorgi, F. Vernejoul, D. Lagorce, L. Buscail, R. Bartenschlager, F. Ichas, R. Rizzuto, and P. Paterlini-Bréchot. 2005. Hepatitis C virus core triggers apoptosis in liver cells by inducing ER stress and ER calcium depletion. Oncogene 24:4921–4933.
6. Blight, K. J., J. A. McKeating, and C. M. Rice. 2002. Highly permissive cell lines for subgenomic and genomic hepatitis C virus RNA replication. J. Virol. 76:13001–13014.
7. Boyce, M., and J. Yuan. 2006. Cellular response to endoplasmic reticulum stress: a matter of life or death. Cell Death Differ. 13:363–373.
8. Brookes, P. S. 2005. Mitochondrial H⁺ leak and ROS generation: an odd couple. Free Radic. Biol. Med. 38:12–23.
9. Calabrese, F., P. Pontisso, E. Pettenazzo, L. Benvegnù, A. Vario, L. Chemello, A. Alberti, and M. Valente. 2000. Liver cell apoptosis in chronic

hepatitis C correlates with histological but not biochemical activity or serum HCV-RNA levels. Hepatology 31:1153–1159.
10. Camacho-Leal, P., and C. P. Stanners. 2008. The human carcinoembryonic antigen (CEA) GPI anchor mediates anoikis inhibition by inactivation of the intrinsic death pathway. Oncogene 27:1545–1553.
11. Chae, Y. J., H. S. Kim, H. Rhim, B. E. Kim, S. W. Jeong, and I. K. Kim. 2001. Activation of caspase-8 in 3-deazaadenosine-induced apoptosis of U-937 cells occurs downstream of caspase-3 and caspase-9 without Fas receptor-ligand interaction. Exp. Mol. Med. 4:284–292.
12. Chiou, H. L., Y. S. Hsieh, M. R. Hsieh, and T. Y. Chen. 2006. HCV E2 may induce apoptosis of Huh-7 cells via a mitochondrial-related caspase pathway. Biochem. Biophys. Res. Commun. 345:453–458.
13. Chou, A. H., H. F. Tsai, Y. Y. Wu, C. Y. Hu, L. H. Hwang, P. I. Hsu, and P. N. Hsu. 2005. Hepatitis C virus core protein modulates TRAIL-mediated apoptosis by enhancing Bid cleavage and activation of mitochondria apoptosis signaling pathway. J. Immunol. 174:2160–2166.
14. Christen, V., S. Treves, F. H. Duong, and M. H. Heim. 2007. Activation of endoplasmic reticulum stress response by hepatitis viruses up-regulates protein phosphatase 2A. Hepatology 46:558–565.
15. Ciccaglione, A. R., C. Marcantonio, A. Costantino, M. Equestre, and M. Rapicetta. 2003. Expression of HCV E1 protein in baculovirus-infected cells: effects on cell viability and apoptosis induction. Intervirology 46:121–126.
16. Ciccaglione, A. R., C. Marcantonio, E. Tritarelli, M. Equestre, F. Magurano, A. Costantino, L. Nicoletti, and M. Rapicetta. 2004. The transmembrane domain of hepatitis C virus E1 glycoprotein induces cell death. Virus Res. 104:1–9.
17. Ciccaglione, A. R., C. Marcantonio, E. Tritarelli, M. Equestre, F. Vendittelli, A. Costantino, A. Geraci, and M. Rapicetta. 2007. Activation of the ER stress gene gadd153 by hepatitis C virus sensitizes cells to oxidant injury. Virus Res. 126:128–138.
18. D'Alessio, M., M. De Nicola, S. Coppola, G. Gualandi, L. Pugliese, C. Cerella, S. Cristofanon, P. Civitareale, M. R. Ciriolo, A. Bergamaschi, A. Magrini, and L. Ghibelli. 2005. Oxidative Bax dimerization promotes its translocation to mitochondria independently of apoptosis. FASEB J. 19:1504–1506.
19. Egger, D., B. Wölk, R. Gosert, L. Bianchi, H. E. Blum, D. Moradpour, and K. Bienz. 2002. Expression of hepatitis C virus proteins induces distinct membrane alterations including a candidate viral replication complex. J. Virol. 76:5974–5984.
20. Elbein, A. D. 1987. Inhibitors of the biosynthesis and processing of N-linked oligosaccharide chains. Annu. Rev. Biochem. 56:497–534.
21. Erdtmann, L., N. Franck, H. Lerat, J. Le Seyec, D. Gilot, I. Cannie, P. Gripon, U. Hibner, and C. Guguen-Guillouzo. 2003. The hepatitis C virus NS2 protein is an inhibitor of CIDE-B-induced apoptosis. J. Biol. Chem. 278:18256–18264.
22. Griffin, S., D. Clarke, C. McCormick, D. Rowlands, and M. Harris. 2005. Signal peptide cleavage and internal targeting signals direct the hepatitis C virus p7 protein to distinct intracellular membranes. J. Virol. 79:15525–15536.
23. Hidajat, R., M. Nagano-Fujii, L. Deng, M. Tanaka, Y. Takigawa, S. Kitazawa, and H. Hotta. 2005. Hepatitis C virus NS3 protein interacts with ELKS-δ and ELKS-α, members of a novel protein family involved in intracellular transport and secretory pathways. J. Gen. Virol. 86:2197–2208.
24. Jarmay, K., G. Karacsony, Z. Ozsvar, I. Nagy, J. Lonovics, and Z. Schaff. 2002. Assessment of histological feature in chronic hepatitis C. Hepatogastroenterology 49:239–243.
25. Jiang, C. C., L. H. Chen, S. Gillespie, K. A. Kiejda, N. Mhaidat, Y. F. Wang, R. Thorne, X. D. Zhang, and P. Hersey. 2007. Tunicamycin sensitizes human melanoma cells to tumor necrosis factor-related apoptosis-inducing ligand-induced apoptosis by up-regulation of TRAIL-R2 via the unfolded protein response. Cancer Res. 67:5880–5888.
26. Jordan, R., L. Wang, T. M. Graczyk, T. M. Block, and P. R. Romano. 2002. Replication of a cytopathic strain of bovine viral diarrhea virus activates PERK and induces endoplasmic reticulum stress-mediated apoptosis of MDBK cells. J. Virol. 76:9588–9599.
27. Kaasik, A., D. Safiulina, A. Zharkovsky, and V. Veksler. 2007. Regulation of mitochondrial matrix volume. Am. J. Physiol. Cell Physiol. 292:C157–C163.
28. Kamada, S., U. Kikkawa, Y. Tsujimoto, and T. Hunter. 2005. Nuclear translocation of caspase-3 is dependent on its proteolytic activation and recognition of a substrate-like protein(s). J. Biol. Chem. 280:857–860.
29. Kim, B. J., S. W. Ryu, and B. J. Song. 2006. JNK- and p38 kinase-mediated phosphorylation of Bax leads to its activation and mitochondrial translocation and to apoptosis of human hepatoma HepG2 cells. J. Biol. Chem. 281:21256–21265.
30. Korenaga, M., T. Wang, Y. Li, L. A. Showalter, T. Chan, J. Sun, and S. A. Weinman. 2005. Hepatitis C virus core protein inhibits mitochondrial electron transport and increases reactive oxygen species (ROS) production. J. Biol. Chem. 280:37481–37488.
31. Kumar, S. 2007. Caspase function in programmed cell death. Cell Death Differ. 14:32–43.
32. Lalier, L., P. F. Cartron, P. Juin, S. Nedelkina, S. Manon, B. Bechinger, and

F. M. Vallette. 2007. Bax activation and mitochondrial insertion during apoptosis. Apoptosis **12:**887–896.

33. Lan, K. H., M. L. Sheu, S. J. Hwang, S. H. Yen, S. Y. Chen, J. C. Wu, Y. J. Wang, N. Kato, M. Omata, F. Y. Chang, and S. D. Lee. 2002. HCV NS5A interacts with p53 and inhibits p53-mediated apoptosis. Oncogene **21:**4801–4811.

34. Lee, A. S. 2001. The glucose-regulated proteins: stress induction and clinical applications. Trends Biochem. Sci. **26:**504–510.

35. Lee, S. H., Y. K. Kim, C. S. Kim, S. K. Seol, J. Kim, S. Cho, Y. L. Song, R. Bartenschlager, and S. K. Jang. 2005. E2 of hepatitis C virus inhibits apoptosis. J. Immunol. **175:**8226–8235.

36. Lee, S. K., S. O. Park, C. O. Joe, and Y. S. Kim. 2007. Interaction of HCV core protein with 14-3-3□ protein releases Bax to activate apoptosis. Biochem. Biophys. Res. Commun. **352:**756–762.

37. Lindenbach, B. D., M. J. Evans, A. J. Syder, B. Wölk, T. L. Tellinghuisen, C. C. Liu, T. Maruyama, R. O. Hynes, D. R. Burton, J. A. McKeating, and C. M. Rice. 2005. Complete replication of hepatitis C virus in cell culture. Science **309:**623–626.

38. Lindenbach, B. D., P. Meuleman, A. Ploss, T. Vanwolleghem, A. J. Syder, J. A. McKeating, R. E. Lanford, S. M. Feinstone, M. E. Major, G. Leroux-Roels, and C. M. Rice. 2006. Cell culture-grown hepatitis C virus is infectious in vivo and can be recultured in vitro. Proc. Natl. Acad. Sci. USA **103:**3805–3809.

39. Lindenbach, B. D., and C. M. Rice. 2005. Unravelling hepatitis C virus replication from genome to function. Nature **436:**933–938.

40. Marusawa, H., M. Hijikata, T. Chiba, and K. Shimotohno. 1999. Hepatitis C virus core protein inhibits Fas- and tumor necrosis factor alpha-mediated apoptosis via NF-κB activation. J. Virol. **73:**4713–4720.

41. Medigeshi, G. R., A. M. Lancaster, A. J. Hirsch, T. Briese, W. I. Lipkin, V. Defilippis, K. Früh, P. W. Mason, J. Nikolich-Zugich, and J. A. Nelson. 2007. West Nile virus infection activates the unfolded protein response, leading to CHOP induction and apoptosis. J. Virol. **81:**10849–10860.

42. Nie, C., C. Tian, L. Zhao, P. X. Petit, M. Mehrpour, and Q. Chen. 2008. Cysteine 62 of Bax is critical for its conformational activation and its pro-apoptotic activity in response to H$_2$O$_2$-induced apoptosis. J. Biol. Chem. **283:**15359–15369.

43. Nomura-Takigawa, Y., M. Nagano-Fujii, L. Deng, S. Kitazawa, K. Ishido, K. Sada, and H. Hotta. 2006. Non-structural protein 4A of Hepatitis C virus accumulates on mitochondria and renders the cells prone to undergoing mitochondria-mediated apoptosis. J. Gen. Virol. **87:**1935–1945.

44. Oliver, F. J., G. de la Rubia, V. Rolli, M. C. Ruiz-Ruiz, G. de Murcia, and J. M. Murcia. 1998. Importance of poly(ADP-ribose) polymerase and its cleavage in apoptosis. J. Biol. Chem. **273:**33533–33539.

45. Pavio, N., P. R. Romano, T. M. Graczyk, S. M. Feinstone, and D. R. Taylor. 2003. Protein synthesis and endoplasmic reticulum stress can be modulated by the hepatitis C virus envelope protein E2 through the eukaryotic initiation factor 2α kinase PERK. J. Virol. **77:**3578–3585.

46. Pawlotsky, J. M., S. Chevaliez, and J. G. McHutchison. 2007. The hepatitis C virus life cycle as a target for new antiviral therapies. Gastroenterology. **132:**1979–1998.

47. Piccoli, C., R. Scrima, G. Quarato, A. D'Aprile, M. Ripoli, L. Lecce, D. Boffoli, D. Moradpour, and N. Capitanio. 2007. Hepatitis C virus protein expression causes calcium-mediated mitochondrial bioenergetic dysfunction and nitro-oxidative stress. Hepatology **46:**58–65.

48. Prikhod'ko, E. A., G. G. Prikhod'ko, R. M. Siegel, P. Thompson, M. E. Major, and J. I. Cohen. 2004. The NS3 protein of hepatitis C virus induces caspase-8-mediated apoptosis independent of its protease or helicase activities. Virology **329:**53–67.

49. Ray, R. B., K. Meyer, R. Steele, A. Shrivastava, B. B. Aggarwal, and R. Ray. 1998. Inhibition of tumor necrosis factor (TNF-α)-mediated apoptosis by hepatitis C virus core protein. J. Biol. Chem. **273:**2256–2259.

50. Safiulina, D., V. Veksler, A. Zharkovsky, and A. Kaasik. 2006. Loss of mitochondrial membrane potential is associated with increase in mitochondrial volume: physiological role in neurones. J. Cell. Physiol. **206:**347–353.

51. Saito, K., K. Meyer, R. Warner, A. Basu, R. B. Ray, and R. Ray. 2006. Hepatitis C virus core protein inhibits tumor necrosis factor alpha-mediated apoptosis by a protective effect involving cellular FLICE inhibitory protein. J. Virol. **80:**4372–4379.

52. Schulze-Osthoff, K., D. Ferrari, M. Los, S. Wesselborg, and M. E. Peter. 1998. Apoptosis signaling by death receptors. Eur. J. Biochem. **254:**439–459.

53. Schwer, B., S. Ren, T. Pietschmann, J. Kartenbeck, K. Kaehlcke, R. Barten-

schlager, T. S. Yen, and M. Ott. 2004. Targeting of hepatitis C virus core protein to mitochondria through a novel C-terminal localization motif. J. Virol. **78:**7958–7968.

54. Scorrano, L., M. Ashiya, K. Buttle, S. Weiler, S. A. Oakes, C. A. Mannella, and S. J. Korsmeyer. 2002. A distinct pathway remodels mitochondrial cristae and mobilizes cytochrome c during apoptosis. Dev. Cell **2:**55–67.

55. Sekine-Osajima, Y., N. Sakamoto, K. Mishima, M. Nakagawa, Y. Itsui, M. Tasaka, Y. Nishimura-Sakurai, C. H. Chen, T. Kanai, K. Tsuchiya, T. Wakita, N. Enomoto, and M. Watanabe. 2008. Development of plaque assays for hepatitis C virus-JFH1 strain and isolation of mutants with enhanced cytopathogenicity and replication capacity. Virology **371:**71–85.

56. Shepard, C. W., L. Finelli, and M. J. Alter. 2005. Global epidemiology of hepatitis C virus infection. Lancet Infect. Dis. **5:**558–567.

57. Siavoshian, S., J. D. Abraham, C. Thumann, M. P. Kieny, and C. Schuster. 2005. Hepatitis C virus core, NS3, NS5A, NS5B proteins induce apoptosis in mature dendritic cells. J. Med. Virol. **75:**402–411.

58. Tanaka, M., M. Nagano-Fujii, L. Deng, S. Ishido, K. Sada, and H. Hotta. 2006. Single-point mutations of hepatitis C virus that impair p53 interaction and anti-apoptotic activity of NS3. Biochem. Biophys. Res. Commun. **340:**792–799.

59. Tardif, K. D., K. Mori, R. J. Kaufman, and A. Siddiqui. 2004. Hepatitis C virus suppresses the IRE1-XBP1 pathway of the unfolded protein response. J. Biol. Chem. **279:**17158–17164.

60. Tardif, K. D., G. Waris, and A. Siddiqui. 2005. Hepatitis C virus, ER stress, and oxidative stress. Trends Microbiol. **13:**159–163.

61. Tewari, M., L. T. Quan, K. O'Rourke, S. Desnoyers, Z. Zeng, D. R. Beidler, G. G. Poirier, G. S. Salvesen, and V. M. Dixit. 1995. Yama/CPP32 beta, a mammalian homolog of CED-3, is a CrmA-inhibitable protease that cleaves the death substrate poly (ADP-ribose) polymerase. Cell **81:**801–809.

62. Thorburn, A. 2004. Death receptor-induced cell killing. Cell. Signal. **16:**139–144.

63. Tsujimoto, Y. 2003. Cell death regulation by the Bcl-2 protein family in the mitochondria. J. Cell. Physiol. **195:**158–167.

64. Upton, J. P., A. J. Valentijn, L. Zhang, and A. P. Gilmore. 2007. The N-terminal conformation of Bax regulates cell commitment to apoptosis. Cell Death Differ. **14:**932–942.

65. Viswanath, V., Y. Wu, R. Boonplueang, S. Chen, F. F. Stevenson, F. Yantiri, L. Yang, M. F. Beal, and J. K. Andersen. 2001. Caspase-9 activation results in downstream caspase-8 activation and bid cleavage in 1-methyl-4-phenyl-1,2,3,6-tetrahydropyridine-induced Parkinson's disease. J. Neurosci. **21:**9519–9528.

66. Wakita, T., T. Pietschmann, T. Kato, T. Date, M. Miyamoto, Z. Zhao, K. Murthy, A. Habermann, H. G. Kräusslich, M. Mizokami, R. Bartenschlager, and T. J. Liang. 2005. Production of infectious hepatitis C virus in tissue culture from a cloned viral genome. Nat. Med. **11:**791–796.

67. Wang, J., W. Tong, X. Zhang, L. Chen, Z. Yi, T. Pan, Y. Hu, L. Xiang, and Z. Yuan. 2006. Hepatitis C virus non-structural protein NS5A interacts with FKBP38 and inhibits apoptosis in Huh7 hepatoma cells. FEBS Lett. **580:**4392–4400.

68. Wei, M. C., W. X. Zong, E. H. Cheng, T. Lindsten, V. Panoutsakopoulou, A. J. Ross, K. A. Roth, G. R. MacGregor, C. B. Thompson, and S. J. Korsmeyer. 2001. Proapoptotic BAX and BAK: a requisite gateway to mitochondrial dysfunction and death. Science **292:**727–730.

69. Yu, C. Y., Y. W. Hsu, C. L. Liao, and Y. L. Lin. 2006. Flavivirus infection activates the XBP1 pathway of the unfolded protein response to cope with endoplasmic reticulum stress. J. Virol. **80:**11868–11880.

70. Zhivotovsky, B., A. Samali, A. Gahm, and S. Orrenius. 1999. Caspases: their intracellular localization and translocation during apoptosis. Cell Death Differ. **6:**644–651.

71. Zhong, J., P. Gastaminza, G. Cheng, S. Kapadia, T. Kato, D. R. Burton, S. F. Wieland, S. L. Uprichard, T. Wakita, and F. V. Chisari. 2005. Robust hepatitis C virus infection in vitro. Proc. Natl. Acad. Sci. USA **102:**9294–9299.

72. Zhu, H., H. Dong, E. Eksioglu, A. Hemming, M. Cao, J. M. Crawford, D. R. Nelson, and C. Liu. 2007. Hepatitis C virus triggers apoptosis of a newly developed hepatoma cell line through antiviral defense system. Gastroenterology **133:**1649–1659.

73. Zhu, N., A. Khoshnan, R. Schneider, M. Matsumoto, G. Dennert, C. Ware, and M. M. C. Lai. 1998. Hepatitis C virus core protein binds to the cytoplasmic domain of tumor necrosis factor (TNF) receptor 1 and enhances TNF-induced apoptosis. J. Virol. **72:**3691–3697.

Hepatitis C virus NS5A protein interacts with and negatively regulates the non-receptor protein tyrosine kinase Syk

Sachiko Inubushi,[1]† Motoko Nagano-Fujii,[1]† Kikumi Kitayama,[1] Motofumi Tanaka,[1] Chunying An,[1] Hiroshi Yokozaki,[2] Hirohei Yamamura,[3] Hideko Nuriya,[4] Michinori Kohara,[4] Kiyonao Sada[1]‡ and Hak Hotta[1]

Correspondence
Hak Hotta
hotta@kobe-u.ac.jp

[1]Division of Microbiology, Kobe University Graduate School of Medicine, Kobe 650-0017, Japan

[2]Division of Surgical Pathology, Kobe University Graduate School of Medicine, Kobe 650-0017, Japan

[3]Hyogo Laboratory, Hyogo Prefectural Institute of Public Health and Environmental Sciences, Kobe 652-0032, Japan

[4]Department of Microbiology and Cell Biology, The Tokyo Metropolitan Institute of Medical Science, Tokyo 113-8613, Japan

Hepatitis C virus (HCV) is the major causative agent of hepatocellular carcinoma. However, the precise mechanism underlying the carcinogenesis is yet to be elucidated. It has recently been reported that Syk, a non-receptor protein tyrosine kinase, functions as a potent tumour suppressor in human breast carcinoma. This study first examined the possible effect of HCV infection on expression of Syk *in vivo*. Immunohistochemical analysis revealed that endogenous Syk, which otherwise was expressed diffusely in the cytoplasm of normal hepatocytes, was localized near the cell membrane with a patchy pattern in HCV-infected hepatocytes. The possible interaction between HCV proteins and Syk in human hepatoma-derived Huh-7 cells was then examined. Immunoprecipitation analysis revealed that NS5A interacted strongly with Syk. Deletion-mutation analysis revealed that an N-terminal portion of NS5A (aa 1–175) was involved in the physical interaction with Syk. An *in vitro* kinase assay demonstrated that NS5A inhibited the enzymic activity of Syk and that, in addition to the N-terminal 175 residues, a central portion of NS5A (aa 237–302) was required for inhibition of Syk. Moreover, Syk-mediated phosphorylation of phospholipase C-γ1 was downregulated by NS5A. An interaction of NS5A with Syk was also detected in Huh-7.5 cells harbouring an HCV RNA replicon or infected with HCV. In conclusion, these results demonstrated that NS5A interacts with Syk resulting in negative regulation of its kinase activity. The results indicate that NS5A may be involved in the carcinogenesis of hepatocytes through the suppression of Syk kinase activities.

INTRODUCTION

Hepatitis C virus (HCV) is the major aetiological agent of viral hepatitis worldwide after hepatitis A and B viruses (Choo *et al.*, 1989), with about 170 million people being infected. The majority of HCV-infected individuals develop chronic infection, which may progress to liver cirrhosis and hepatocellular carcinoma (HCC). HCV is a member of the family *Flaviviridae* and its genome consists of a single-stranded, positive-sense RNA of approximately

9600 nt, which encodes a polyprotein precursor of about 3010 aa. Currently, clinical HCV isolates are classified into six genotypes and more than 60 subtypes (Doi *et al.*, 1996; Mellor *et al.*, 1995; Robertson *et al.*, 1998). The polyprotein is cleaved by signal peptidase, signal peptide peptidase and two virally encoded proteases to generate at least ten mature proteins: core, envelope glycoprotein 1 (E1), E2, p7, non-structural protein 2 (NS2), NS3, NS4A, NS4B, NS5A and NS5B (Okamoto *et al.*, 2004; Reed & Rice, 2000).

HCV NS5A is part of the replication complex that catalyses replication of the viral genome. NS5A takes two forms, p56 and p58, with different degrees of phosphorylation, which may play distinct roles in the virus replication cycle (Evans

---

†These authors contributed equally to this work.

‡Present address: Division of Microbiology, Department of Pathological Sciences, Faculty of Medical Sciences, University of Fukui, Fukui 910-1193, Japan.

et al., 2004; Song et al., 1999). The SNARE-like membrane fusion proteins VAP-A and VAP-B have been reported to interact with NS5A, and the binding capacity is inversely correlated to the degree of NS5A phosphorylation (Evans et al., 2004; Gao et al., 2004; Hamamoto et al., 2005). NS5A binds to and inhibits double-stranded RNA-dependent protein kinase (PKR) (Gale et al., 1998) and 2',5'-oligoadenylate synthetase (Taguchi et al., 2004). NS5A seems to have the potential to regulate not only interferon responses but also many other cellular functions, such as mitogenic signalling, apoptosis, the cell cycle and reactive oxygen species signalling, by interacting with a variety of host proteins (Macdonald et al., 2004). These NS5A-interacting proteins include SRCAP (Ghosh et al., 2000), Grb2 (He et al., 2002; Tan et al.,1999), p53 (Majumder et al., 2001; Qadri et al., 2002), phosphatidylinositol 3-kinase p85 subunit (He et al., 2002; Street et al., 2004), karyopherin β3 (Chung et al., 2000), apolipoprotein A1 (Shi et al., 2002), amphiphysin II (Zech et al., 2003) and Src family protein tyrosine kinases (Macdonald & Harris, 2004; Macdonald et al., 2004).

The non-receptor protein tyrosine kinase Syk is widely expressed in cells of the haematopoietic lineage, endothelium, epithelium and hepatocytes (Coopman et al., 2000; Sada et al., 2001; Tsuchida et al., 2000; Turner et al., 2000; Yanagi et al., 1995, 2001). Syk contains tandem SH2 and kinase domains that are connected by an inter-SH2 domain and a linker region (Taniguchi et al., 1991). The tandem SH2 domains of Syk bind to diphosphorylated immunoreceptor tyrosine-based activation motifs [ITAMs: $YXX(L/I)X_{6-8}YXX(L/I)$] in the cytoplasmic tail of the Fc receptor γ-chain or B-cell receptor subunit Igα to be activated after the engagement of immune receptors (Kurosaki et al., 1995; Sada et al., 2001; Shiue et al., 1995; Turner et al., 1995; Weiss & Littman, 1994). Autophosphorylation of Syk on Tyr^{525} and Tyr^{526} in the activation loop of the kinase domain results in an increase in its intrinsic kinase activity to phosphorylate its downstream signalling molecules, such as phospholipase C (PLC)-γ (Kurosaki et al., 1995). Autophosphorylation on Tyr^{352} in the linker region is required for tyrosine phosphorylation of PLC-γ1 (Law et al., 1996). Genetic studies have demonstrated that Syk is required for the development and maturation of B cells, mast-cell activation and platelet aggregation (Cheng et al., 1995; Costello et al., 1996; Poole et al., 1997; Turner et al., 1995, 2000). Furthermore, it has been reported that Syk functions as a tumour suppressor in breast cancers and that loss of Syk expression appears to be associated with malignant phenotypes (Coopman et al., 2000).

In the present study, we demonstrated that HCV NS5A interacts physically with Syk to inhibit its kinase activity in human hepatoma-derived Huh-7 cells. Our results indicate that NS5A-induced downregulation of the possible tumour suppressor Syk may play a role in malignant transformation of HCV-infected hepatocytes.

METHODS

Expression plasmids. Mammalian expression plasmids for each of the Myc-tagged HCV proteins were constructed by amplifying and subcloning the corresponding cDNA fragments of pFK5B/2884Gly (Lohmann et al., 2001) in frame to the pEF1/Myc-His(−) vector (Invitrogen). pFK5B/2884Gly was a kind gift from Dr R. Bartenschlager (University of Heidelberg, Germany). An expression plasmid for a polyprotein consisting of NS3–NS5B was amplified from pFK5B/2884Gly and subcloned into pEF1/Myc-His(−). Deletion mutants of NS5A were also amplified by PCR and subcloned into pEF1/Myc-His(−). Point mutations in NS5A [Tyr^{118} to Phe (Y118F), Val^{121} to Ala (V121A)] were introduced into pEF1/NS5A-Myc-His(−) by site-directed mutagenesis. Human Syk cDNA was a gift from Dr B. Müller-Hilke (University of Rostock, Germany). cDNA fragments for FLAG-tagged truncated forms and the kinase-inactive form of Syk were generated by PCR. All mutant forms of FLAG-tagged Syk were subcloned into pcDNA3.1/Hygro(+) (Invitrogen).

Cells, HCV RNA replicon and virus. Huh-7 human hepatoma-derived cells were maintained in Dulbecco's modified Eagle's medium supplemented with 10 % heat-inactivated fetal calf serum (FCS). Huh-7.5 cells (Blight et al., 2002) were kindly provided by Dr C. M. Rice (The Rockefeller University, USA). BJAB cells, a human B-cell line expressing endogenous Syk, were cultured in RPMI 1640 supplemented with 10 % FCS.

Huh-7.5 cells stably harbouring an HCV subgenomic RNA replicon were prepared by using pFK5B/2884Gly, as described previously (Hidajat et al., 2005; Lohmann et al., 2001; Taguchi et al., 2004; Takigawa et al., 2004).

The plasmid pFL-J6/JFH1 encoding the entire genome of the HCV J6/JFH-1 strain was kindly provided by Dr C. M. Rice, and cell-free virus was propagated in Huh-7.5 cell cultures, as described previously (Lindenbach et al., 2005).

Protein expression. Protein expression was performed using a recombinant vaccinia virus expressing T7 RNA polymerase (vTF7-3), as described previously (Deng et al., 2006; Muramatsu et al., 1997). In some experiments, protein expression was performed using a plasmid-based expression system without vTF7-3. For BJAB cells, we used an electroporation method (Schneider & Kieser, 2004). In brief, 3×10^6 cells were washed once with PBS and incubated for 10 min with 15 µg plasmid DNA in 250 µl RPMI 1640. Electroporation was carried out in a 4 mm cuvette using a Bio-Rad Gene Pulser II with a capacity of 975 µF and a voltage of 180 V. Immediately after electroporation, 500 µl FCS was added to the cells, which were then transferred to 4.5 ml RPMI 1640.

To activate Syk under hyperosmolarity conditions, cells were incubated with serum-free medium containing 400 mM sorbitol for 30 min at 37 °C, as described previously (Miah et al., 2004). In addition, cells were treated with sodium pervanadate (generated by mixing 0.1 mM Na_3VO_4 with 1 mM H_2O_2) for 30 min to activate Syk (Wienands et al., 1996).

Immunohistochemistry. Human normal adult liver autopsy materials and surgically resected liver tissue of patients with HCV-associated HCC were obtained with written informed consent. The tissues were fixed with 10 % buffered formalin, embedded in paraffin and sectioned. Immunohistochemical staining was performed with a Dako EnVision+ kit, according to the manufacturer's instructions. In brief, fixed sections were depleted of paraffin by treatment with xylene, dehydrated in ethanol and incubated with 3 % H_2O_2 to quench endogenous peroxidase activity. After being autoclaved at 121 °C for 20 min, the sections were incubated with a blocking

solution and then with anti-Syk rabbit polyclonal antibody (N-19; Santa Cruz Biotech). Normal rabbit IgG served as a control. The sections were then incubated with horseradish peroxidase-labelled polymer-conjugated secondary antibody. The sections were counter-stained with haematoxylin and examined under a light microscope. To confirm the specificity of immunostaining, anti-Syk antibody was pre-incubated with a 1000-fold excess of blocking peptide (Santa Cruz Biotech) for 2 h at room temperature prior to staining.

Detection of HCV RNA by *in situ* RT-PCR. *In situ* RT-PCR was performed as described previously (Maeda *et al.*, 2004) with some modifications. Briefly, OCT-embedded frozen liver biopsy sections were fixed with 10 % formaldehyde and treated with proteinase K. The samples were subjected to *in situ* reverse transcription using Moloney murine leukemia virus reverse transcriptase with an antisense primer for HCV (nt 290–272; 5'-AGTACCACAA GGCCTTTCG-3'), followed by *in situ* PCR using an *in situ* PCR System 1000 (Applied Biosystems) in the reaction mixture containing the antisense and a sense primer (nt 129–147; 5'-CCGGGAGAG CCATAGTGGT-3'). After being fixed in 4 % paraformaldehyde, the PCR products were detected by *in situ* hybridization using a digoxigenin (DIG)-labelled oligonucleotide probe, 5'-(DIG)-ATTTGGGCTGTGCCCCCGCGAGACTGCTAGCCGAGTAGTGTT-GGGT-(DIG)$_n$-3' (nt 225–270). Anti-DIG antibody conjugated with alkaline phosphatase (Roche) was used to detect the probe. The slides were incubated in a dye solution containing nitro blue tetrazolium, 5-bromo-4-chloro-3-indolylphosphate and levamizole to yield a purplish-blue precipitate.

Immunoprecipitation and Western blotting. Cultured cells were lysed with a buffer containing 1 % Triton X-100, 50 mM Tris/HCl (pH 7.4), 150 mM NaCl, 10 mM EDTA, 1 mM NaF, 1 mM Na$_3$VO$_4$ and 1 mM PMSF. The lysate was centrifuged at 12 000 *g* for 20 min at 4 °C and the supernatant was immunoprecipitated with appropriate antibodies. In the case of liver tissue, each tissue sample was placed in a tube containing glass beads (1 mm diameter; BioSpec Products) to which 1 ml lysis buffer was added. The tube was then shaken at 4 °C for 3 min using a Mini-BeadBeater (BioSpec Products) to homogen-ize the tissues. After centrifugation at 80 *g* for 3 min, the supernatant was collected for immunoprecipitation analysis.

Immunoprecipitation and Western blot analyses were performed as described previously (Deng *et al.*, 2006). In brief, the supernatants of the lysates were pre-cleared with control IgG and protein A–Sepharose 4 Fast Flow (GE Healthcare) and incubated with appropriate antibodies at 4 °C for 1 h, followed by incubation with protein A–Sepharose 4 Fast Flow for another 1 h. After six washes with lysis buffer, the immunoprecipitates were analysed by Western blotting.

Antibodies used were as follows: anti-FLAG rabbit polyclonal antibody (Sigma); anti-Myc polyclonal and monoclonal antibodies (Santa Cruz Biotech); anti-Syk monoclonal antibody (4D10; Santa Cruz Biotech); anti-phospho Syk(Tyr^{352}) and Syk(Tyr$^{525/526}$) rabbit polyclonal antibodies (Cell Signaling Technology); anti-PLC-γ1 monoclonal antibody (BD Biosciences); mouse monoclonal antibod-ies against core (Yasui *et al.*, 1998), NS3, NS4A and NS5A (kind gifts from Dr I. Fuke, Osaka University, Japan); anti-NS5A rabbit polyclonal antibody (NS5ACL1; a kind gift from Dr K. Shimotohno, Kyoto University, Japan; Miyanari *et al.*, 2007); and anti-NS5B goat polyclonal antibody (sc-17532; Santa Cruz Biotech). Normal IgG served as a control.

***In vitro* protein kinase assay.** An *in vitro* protein kinase assay was performed as reported previously (Miah *et al.*, 2004; Sada *et al.*, 2000, 2001). In brief, immunoprecipitates obtained with anti-Syk antibody from differentially transfected cells were incubated with 10 μg H2B histone (Sigma) as substrate in 20 μl kinase buffer, composed of
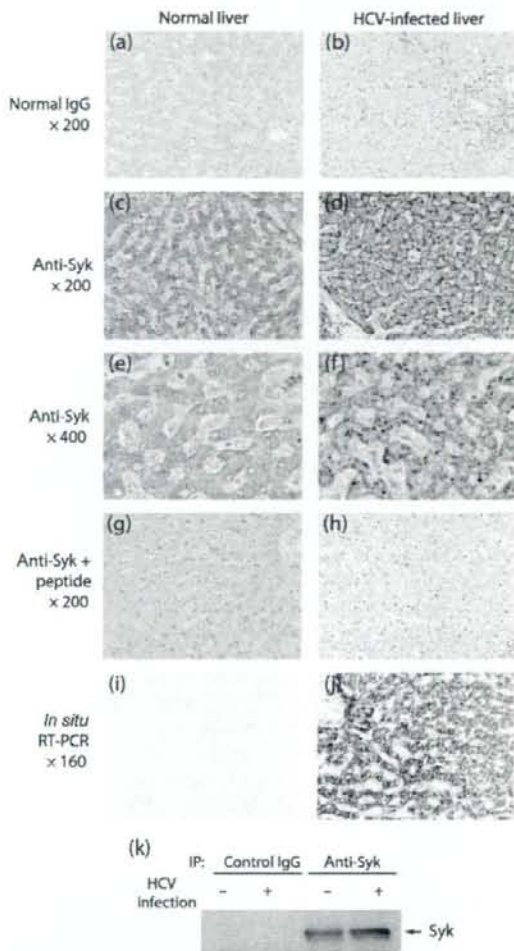
Fig. 1. Endogenous Syk expression in human liver tissues *in vivo*. Normal liver tissues (a, c, e, g, i) and HCV-infected non-cancerous liver tissues (b, d, f, h, j) were analysed. Formalin-fixed samples were stained with control IgG (a, b) or anti-Syk polyclonal antibody without (c–f) or with (g, h) pre-incubation with an excess amount of the immunogenic peptides. Frozen tissues were sectioned and examined for the presence of HCV RNA by *in situ* RT-PCR (i, j). Representative results are shown from four normal livers and ten HCV-infected livers. (k) Western blot analysis of normal human liver and HCV-infected non-cancerous liver. Supernatants of liver tissue homogenates (1.75 mg protein equivalent) were immuno-precipitated with anti-Syk monoclonal antibody (4D10) and probed with the same antibody or with control IgG.

30 mM HEPES (pH 7.5), 10 mM MgCl$_2$, 2 mM MnCl$_2$, 4 μM ATP and 4 μCi (148 kBq) [γ-^{32}P]ATP, for 30 min at room temperature. Reactions were terminated by boiling for 5 min in 2 × sample buffer.

Proteins were separated by SDS-PAGE. The gels were treated with 1 M KOH for 1 h at 56 °C to remove phosphoserine and most of the phosphothreonine. After gel drying, radiolabelled proteins were visualized by autoradiography. For quantitative analysis, γ-^{32}P incorporation was measured using a PhosphorImager (BAS2000; Fuji) and protein amounts with an LAS1000 image analyser (Fuji).

RESULTS

### Different expression patterns of endogenous Syk in normal and HCV-infected liver tissues

We first examined whether Syk was expressed in human liver tissues. Immunohistochemical analysis revealed that Syk was indeed expressed and rather diffusely distributed throughout the cytoplasm of normal adult hepatocytes (Fig. 1c, e). This pattern was observed with four out of four normal liver tissues (100 %; data not shown). The specificity of the staining was verified by pre-incubating the antibody with an excess amount of the immunogenic peptides (Fig. 1g, h). We then examined Syk expression in non-cancerous liver tissue obtained from patients with HCV-associated HCC. Interestingly, Syk was detected near the plasma membrane with a patchy pattern in hepatocytes of eight out of ten HCV-infected patients (80 %; Fig. 1d, f, and data not shown). All of the specimens stained with normal rabbit IgG were negative (Fig. 1a, b). We confirmed that almost all of the hepatocytes in the tissue samples were infected with HCV using *in situ* RT-PCR (Fig. 1i, j).

Western blot analysis confirmed Syk expression in human liver tissue, irrespective of HCV infection (Fig. 1k). It should be noted, however, that the Syk expression was rather weak, as we could achieve successful Western blotting only after the tissue lysates were concentrated by immunoprecipitation with specific antibody. Also, possibly due to the low level of expression and comparatively low sensitivity of the antibodies used for Western blotting, we could not detect the phosphorylated forms of Syk in the liver tissue (data not shown).

### Identification of Syk as a novel NS5A-interacting protein

We then examined the possible interaction between HCV proteins and Syk in cultured cells. For this purpose, various HCV proteins and Syk were expressed ectopically in Huh-7 cells, as these cells do not express endogenous Syk. Co-immunoprecipitation analysis revealed that NS5A associated with Syk, whereas the other HCV proteins associated with Syk very weakly or not at all (Fig. 2a, b). A specific interaction of NS5A with Syk was also observed when NS5A was expressed as part of an NS3–NS5B polyprotein (Fig. 2c). These results collectively suggested that NS5A interacts specifically with Syk.

Next, we examined the possible interaction of NS5A with endogenously expressed Syk. As human hepatoma-derived cell lines, such as Huh-7, HepG2 and FLC4, are negative for
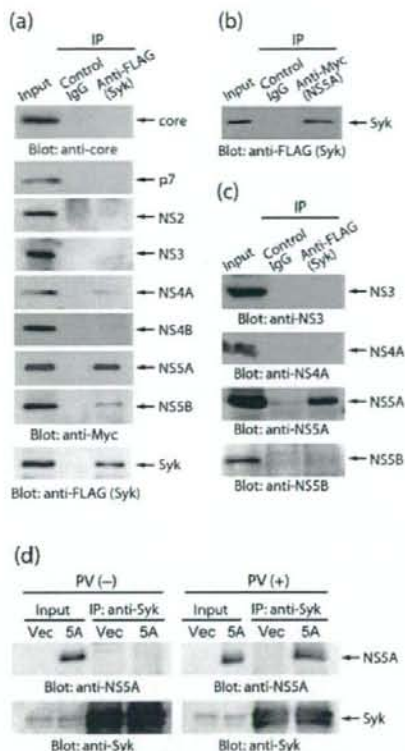
Fig. 2. NS5A specifically interacts with Syk in Huh-7 cells. (a) Each of the Myc-tagged HCV proteins was expressed with FLAG-tagged full-length Syk. Cell lysates were immunoprecipitated using anti-FLAG antibody or control IgG. Cell lysates (input) and the immunoprecipitates were probed with anti-core or anti-Myc antibodies. A representative result verifying efficient immunoprecipitation is shown at the bottom. (b) Myc-tagged NS5A was expressed with FLAG-tagged full-length Syk. Cell lysates were immunoprecipitated using anti-Myc antibody or control IgG, and probed with anti-FLAG antibody. (c) A polyprotein consisting of NS3–NS5B was expressed with FLAG-tagged Syk. Cell lysates were immunoprecipitated with anti-FLAG antibody or control IgG, and probed with the indicated antibodies. (d) NS5A was expressed in BJAB cells expressing endogenous Syk. The cells were treated with pervanadate (PV) or left untreated. Cell lysates were immunoprecipitated with anti-Syk monoclonal antibody and probed with anti-NS5A or anti-Syk monoclonal antibody. Vec, control using empty vector.

endogenous Syk expression, we used BJAB cells endogenously expressing Syk. Unlike ectopically expressed Syk, endogenous Syk in BJAB cells is not tyrosine phosphorylated. Therefore, we treated the cells with pervanadate to induce tyrosine phosphorylation of Syk. Co-immunoprecipitation experiments clearly demonstrated that NS5A
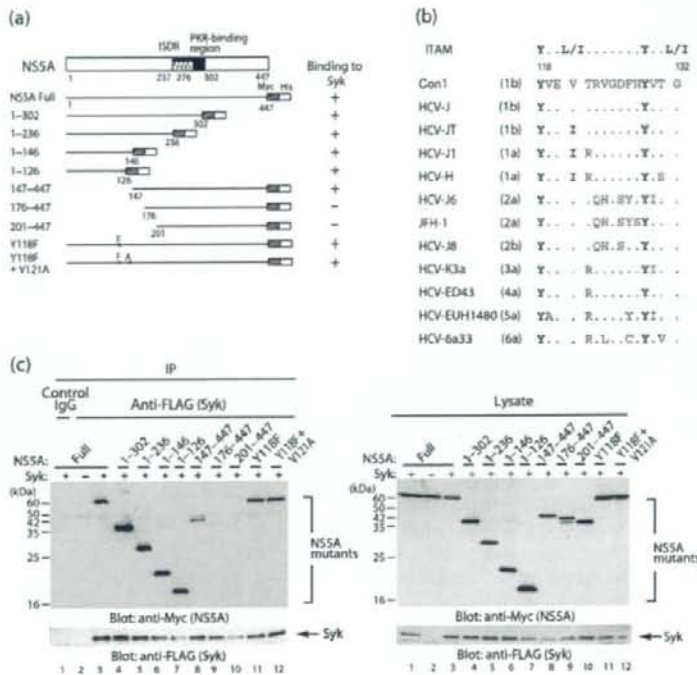
Fig. 3. Determination of the Syk-binding region(s) of NS5A. (a) Schematic diagram of various deletion mutants of NS5A and their Syk-binding capacity. (b) Alignment of amino acid sequences surrounding the ITAM-related sequence in NS5A of various HCV strains. The genotype is indicated in parentheses. Residues identical to those of HCV strain Con1 are shown by a dot. Residues identical to ITAM are shown in bold. (c) Full-length (Full) and a series of deletion mutants of Myc-tagged NS5A were expressed in Huh-7 cells with or without FLAG-tagged full-length Syk. Cell lysates were immunoprecipitated using anti-FLAG antibody and probed with anti-Myc antibody (left panel). Efficient immunoprecipitation was verified (bottom). Cell lysates were probed directly with anti-Myc and anti-FLAG antibodies to verify comparable expression levels of the NS5A mutants and Syk, respectively (right panels).

interacted with endogenous Syk when the cells were treated with pervanadate, but not when the cells were left untreated (Fig. 2d).

The N-terminal region of NS5A is required for interaction with Syk

To map a Syk-interacting region(s) of NS5A, interaction between various deletion mutants of NS5A and Syk was tested. C-terminally deleted mutants of NS5A up to aa 126, as well as the full-length NS5A, were co-immunoprecipitated with Syk (Fig. 3a, c). This result suggested that neither the PKR-binding region nor the interferon sensitivity-determining region (ISDR) of NS5A was required for the interaction with Syk. A proline-rich region of NS5A (aa 343–356), which is reported to bind to the Src family kinases (Macdonald & Harris, 2004; Macdonald et al., 2004), was not involved in the Syk interaction either. In contrast, the N-terminally truncated

mutant of NS5A(147–447), but not the further truncated mutants NS5A(176–447) or NS5A(201–447), was co-immunoprecipitated with Syk, suggesting that a region of NS5A between aa 147 and 175 is also involved in the interaction with Syk. We also observed that NS5A(1–126) and NS5A(174–447), but not NS5A(201–447), interacted with Syk(1–261) or Syk(379–635) (data not shown). These results collectively suggested that NS5A interacts with Syk through two independent regions of NS5A (aa 1–126 and 147–175).

Syk is activated by interaction with a diphosphorylated ITAM of immune receptors (Sada et al., 2001; Turner et al., 2000; Weiss & Littman, 1994). NS5A from HCV strain Con1 possesses a sequence (AEEY^{118}VEV^{121}-TRVGDFHY^{129}VTG) that resembles an ITAM (Fig. 3b). We found that the two tyrosine residues at positions 118 and 129 are highly conserved across different genotypes and subtypes. The tyrosine at position 118 is exposed on

–168–
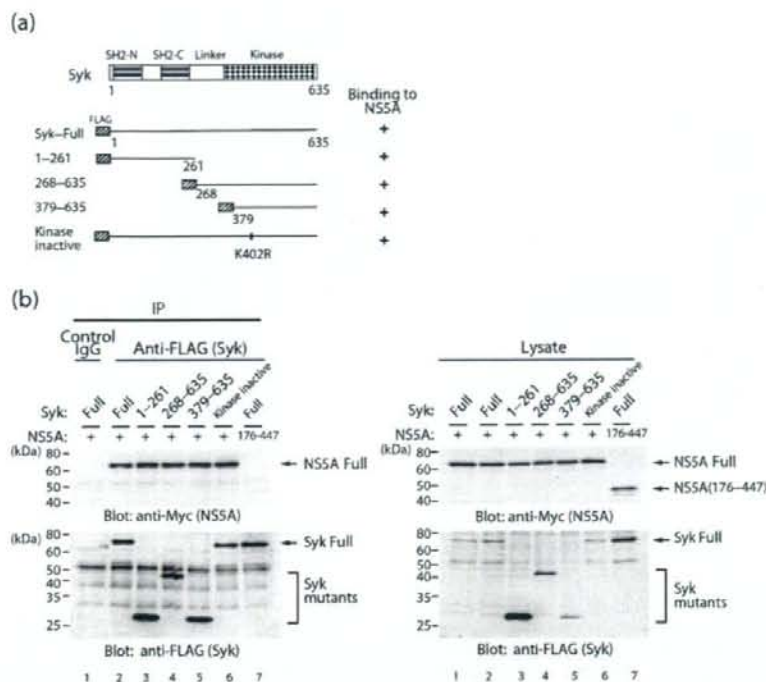
Fig. 4. NS5A interacts with both N-terminal and C-terminal regions of Syk. (a) Schematic diagram of the deletion mutants of Syk and their NS5A-binding capacity. (b) Full-length (Full) and a series of domain-deletion mutants of FLAG-tagged Syk was expressed in Huh-7 cells with Myc-tagged full-length NS5A (lanes 1–6) or NS5A(176–447) (lane 7). Cell lysates were immunoprecipitated using anti-FLAG antibody and probed with anti-Myc antibody (left upper panel). Efficient immunoprecipitation of Syk deletion mutants was verified (bottom). Cell lysates were probed directly with anti-Myc and anti-FLAG antibodies to verify comparable expression levels of the NS5A and Syk mutants, respectively (right panels).

the surface of the NS5A molecule (Tellinghuisen *et al.*, 2005). We examined whether this sequence motif was involved in the interaction with Syk. A single point mutation of Tyr[118] (Y118F) or double mutations of Tyr[118] and Val[121] (Y118F and V121A) in NS5A did not affect the interaction with Syk (Fig. 3c, lanes 11 and 12). Thus, it is unlikely that NS5A binds to Syk through its ITAM-related sequence in the same manner as that observed for immune receptors.

To map the NS5A-binding region in Syk, a series of domain-deleted mutants of Syk was examined. The results obtained revealed that both N-terminal (tandem SH2 domains) and C-terminal halves (linker and the kinase domain) interacted with NS5A (Fig. 4). The kinase domain alone and a kinase-inactive form of Syk were also co-immunoprecipitated with NS5A. These results suggested that the NS5A–Syk interaction occurs through the N- and C-terminal regions of Syk and that the catalytic activity of Syk is not necessary for the interaction.

NS5A expression downregulates the kinase activity of Syk

Next, we tested the possible effect of NS5A expression on Syk kinase activity. An *in vitro* kinase assay revealed that full-length NS5A and a C-terminally deleted NS5A(1–302) mutant significantly inhibited Syk kinase activity (Fig. 5, lanes 2–4). In contrast, NS5A(1–236), which lacked both the PKR-binding region (aa 237–302) and ISDR (aa 237–276), failed to inhibit Syk kinase activity, although it could interact with Syk. NS5A(176–447), which contained the PKR-binding region and ISDR but lacked the Syk-binding region, did not affect Syk kinase activity. These results collectively suggested that NS5A requires both N-terminal (aa 1–175) and central (aa 237–302) regions for the downregulation of Syk kinase activity (Table 1).

To address the relevance of the interaction between NS5A and Syk, the possible effect(s) of NS5A on Syk-mediated cellular signalling in Huh-7 cells was examined. Ectopic
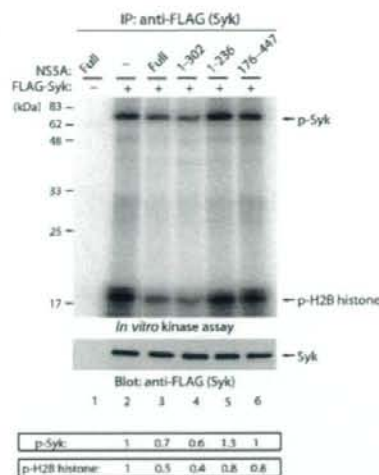
Fig. 5. NS5A downregulates Syk kinase activity. Myc-tagged NS5A and FLAG-tagged Syk were expressed in Huh-7 cells. Cell lysates were immunoprecipitated with anti-FLAG antibody and the immunoprecipitates were subjected to an *in vitro* kinase assay using H2B histone as substrate. Phosphorylation of Syk (p-Syk) and H2B histone (p-H2B histone) was visualized by autoradiography (upper panel). Efficient immunoprecipitation of Syk was verified (lower panel). Arbitrary units of Syk kinase activities, represented by the phosphorylation values of p-Syk and p-H2B histone normalized to the amounts of immunoprecipitated Syk, are shown at the bottom.

Table 1. Summary of NS5A deletion mutational analysis of the interaction with Syk and inhibition of Syk kinase activity

NS5A mutant	Interaction with Syk	Inhibition of Syk
NS5A(1–447; full)	+	+
NS5A(1–302)	+	+
NS5A(1–236)	+	−
NS5A(176–447)	−	−

NS5A expressed in the context of HCV RNA replication interacts with Syk in Huh-7.5 cells

The interaction of NS5A with Syk was examined further using Huh-7.5 cells harbouring an HCV subgenomic RNA replicon. The results obtained clearly demonstrated that NS5A expressed in the context of HCV RNA replication interacted with Syk (Fig. 7a). It is well known that NS5A takes two forms, p56 and p58, with the former being the basally phosphorylated form and the latter the hyperphosphorylated form (Kaneko *et al.*, 1994; Song *et al.*, 1999). It is noteworthy that Syk interacted with p56 more efficiently than with p58.
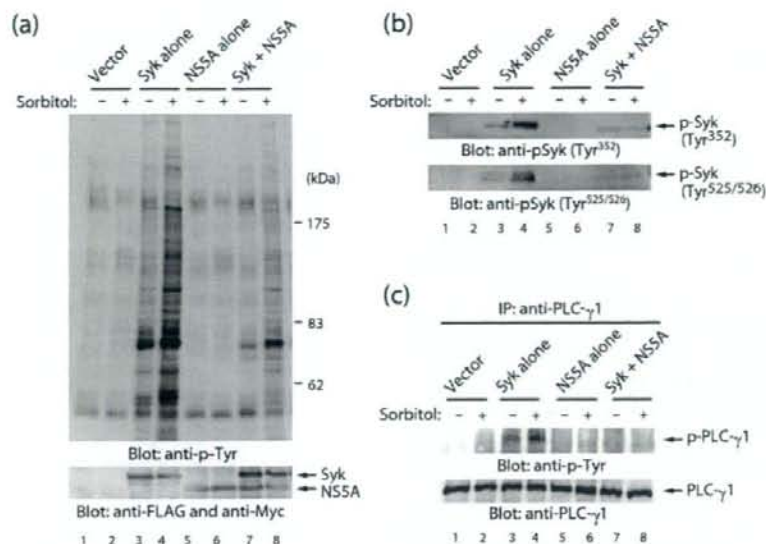
We also examined the interaction of NS5A with Syk in Huh-7.5 cells infected with the J6/JFH-1 strain of HCV. The results demonstrated that NS5A interacted with Syk in HCV-infected cells (Fig. 7b). These results collectively suggested that the NS5A–Syk interaction occurs in the context of virus replication, where NS5A is primarily utilized to form the viral replication complex. In this connection, HCV J6/JFH-1 replication was not affected significantly by ectopically expressed Syk in Huh-7.5 cells (data not shown). This observation, however, does not necessarily exclude the possibility that the NS5A interaction with Syk exerts certain biological effect(s) on the host cell's fate.

Syk kinase activity is suppressed in the context of HCV RNA replication

We then examined Syk kinase activity in the HCV subgenomic RNA-harbouring Huh-7.5 cells. An *in vitro* kinase assay demonstrated that Syk kinase activities, represented by autophosphorylation of Syk (p-Syk) and phosphorylation of a substrate (p-H2B histone), were significantly suppressed in HCV RNA-replicating cells compared with the control (Fig. 7c). These results suggested the possibility that Syk kinase activity is downregulated through an NS5A–Syk interaction in HCV-infected hepatocytes as well.

DISCUSSION

The non-receptor protein tyrosine kinase Syk is expressed in a wide variety of haematopoietic cell lineages (Taniguchi *et al.*, 1991). It is also expressed in human mammary

expression of Syk alone mediated signal transduction to induce tyrosine phosphorylation of a wide variety of cellular proteins, either directly or indirectly (Fig. 6a, lanes 1 and 3). Hyperosmolarity stress (400 mM sorbitol treatment) enhanced Syk-mediated tyrosine phosphorylation of cellular proteins (Fig. 6a, lanes 3 and 4), with the result being consistent with the previous observation (Miah *et al.*, 2004). Interestingly, co-expression of NS5A decreased Syk-mediated tyrosine phosphorylation of cellular proteins both in the absence and presence of hyperosmolarity stress (Fig. 6a, lanes 7 and 8). The phosphorylation of Syk on Tyr^{352} and/or $Tyr^{525/526}$ is a marker for Syk activation. Using these parameters, we confirmed that co-expression of NS5A inhibited Syk activation both in the absence and presence of hyperosmolarity stress (Fig. 6b).

PLC-γ1 has been reported to be a downstream molecule of Syk-mediated signal transduction (Law *et al.*, 1996). Our results demonstrated that NS5A inhibited PLC-γ1 phosphorylation, probably through downregulation of Syk kinase activity, both in the absence and presence of hyperosmolarity stress (Fig. 6c).

Fig. 6. NS5A suppresses hyperosmolarity stress-induced Syk-mediated tyrosine phosphorylation of cellular proteins. (a) Myc-tagged NS5A was expressed in Huh-7 cells with or without FLAG-tagged Syk. The cells were incubated with or without 400 mM sorbitol for 30 min and then lysed in lysis buffer. Half of the cell lysate was probed with anti-phosphotyrosine (p-Tyr) antibody (upper panel) and the remaining half with anti-FLAG and anti-Myc antibodies (bottom). (b) Cell lysates were probed with anti-p-Syk(Tyr^{352}) (upper panel) or anti-p-Syk(Tyr$^{525/526}$) antibody (lower panel). (c) Cell lysates were immunoprecipitated using anti-PLC-γ1 antibody and probed with anti-p-Tyr antibody (upper panel). Efficient immunoprecipitation of PLC-γ1 was verified (lower panel).

(Coopman et al., 2000) and airway epithelial cells (Ulanova et al., 2005), nasal fibroblasts (Yamada et al., 2001) and hepatocytes (Tsuchida et al., 2000). These results suggest that Syk plays a general physiological role in non-haematopoietic cells as well. The first report of Syk having a role in cancer was a study of mammary epithelial cells (Coopman et al., 2000). Since then, there have been several reports that Syk functions as a tumour suppressor in the process of malignant tumour development, such as gastric cancer (Wang et al., 2004) and leukaemia (Goodman et al., 2001). To look into the possible relevance of Syk in HCV-infected hepatocytes and also the possible involvement of Syk in HCC development, we first examined Syk expression in hepatocytes obtained from HCV-infected and uninfected subjects. We found that Syk was expressed near the plasma membrane of hepatocytes of HCV-infected patients, with a patchy pattern, whereas it was expressed rather diffusely in the cytoplasm of normal, uninfected hepatocytes (Fig. 1).

We also demonstrated that NS5A interacted with Syk and inhibited its kinase activity when expressed ectopically in Huh-7 cells (Figs 2, 5 and 6). The NS5A interaction with Syk was observed even in the context of HCV RNA replication (Fig. 7a, b) and Syk kinase activity was inhibited

in HCV RNA replicon-harbouring cells (Fig. 7c). It is likely, therefore, that Syk is a binding partner of NS5A and is functionally inhibited in HCV-infected hepatocytes as well. Whilst an N-terminal portion of NS5A (aa 1–175) was responsible for the binding to Syk, a central portion (aa 237–302) was also required for the inhibition of Syk kinase activity (Figs 3 and 5). It has been reported that NS5A associates with the non-receptor protein tyrosine kinases Lyn and Fyn, members of the Src family kinases, through the proline-rich region of NS5A (aa 343–356) and the SH3 domain of the kinases, thereby inhibiting and activating the kinase activities of Lyn and Fyn, respectively (Macdonald & Harris, 2004; Macdonald et al., 2004). In contrast, Syk does not possess an SH3 domain but has two tandem SH2 domains. These SH2 domains are known to interact with diphosphorylated ITAM of immune receptors, resulting in activation of Syk in an autocrine or paracrine manner (Sada et al., 2001; Yanagi et al., 1995). However, it is unlikely that the NS5A–Syk interaction occurs through its ITAM-related sequence in the same manner as that observed for immune receptors, as NS5A mutants with a mutated ITAM-like sequence still interacted with Syk (Fig. 3). Also, the SH2 domains of Syk are not the only binding sites for NS5A (Fig. 4). These results suggest that the mechanism
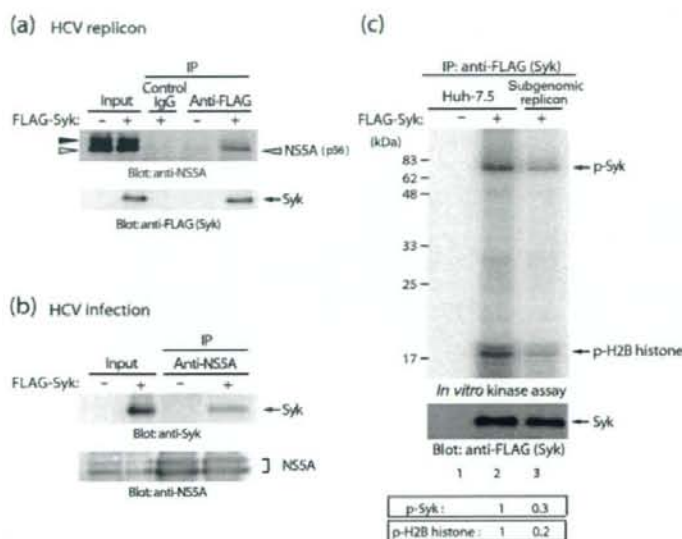
Fig. 7. NS5A expressed in the context of HCV RNA replication interacts with Syk and inhibits its kinase activity. (a) FLAG-tagged Syk was expressed in HCV RNA replicon-harbouring Huh-7.5 cells. Cell lysates were immunoprecipitated with anti-FLAG antibody or control IgG and probed with anti-NS5A (upper panel) or anti-FLAG antibody (lower panel). Filled and open arrowheads indicate the hyperphosphorylated (p58) and hypophosphorylated forms of NS5A (p56), respectively. (b) FLAG-tagged Syk was expressed in HCV J6/JFH-1-infected Huh-7.5 cells. Cell lysates were immunoprecipitated with anti-NS5A polyclonal antibody and probed with anti-Syk monoclonal antibody. (c) FLAG-tagged Syk was expressed in HCV RNA replicon-harbouring Huh-7.5 cells. Cell lysates were immunoprecipitated with anti-FLAG antibody and the immunoprecipitates were subjected to an *in vitro* kinase assay using H2B histone as substrate. Phosphorylation of Syk (p-Syk) and H2B histone (p-H2B histone) was visualized by autoradiography (upper panel). Efficient immunoprecipitation of Syk was verified (lower panel). Arbitrary units of Syk kinase activities, represented by the phosphorylation values of p-Syk and p-H2B histone normalized to the amounts of immunoprecipitated Syk, are shown at the bottom.

underlying the NS5A–Syk interaction differs from what has been observed for Syk and its interacting proteins in immune cells. It is possible that multiple regions of NS5A are involved in the interaction with Syk. Alternatively, NS5A may interact with Syk indirectly through the other host protein(s) that binds directly to Syk.

Syk is activated by cytokine stimulation, hyperosmolarity shock, oxidative stress and engagement with integrin (Corey *et al.*, 1994; Gao *et al.*, 1997; Miah *et al.*, 2004). However, the biological relevance of Syk in hepatocytes has not yet been demonstrated. We have shown in the present study that hyperosmolarity stress-induced activation of Syk resulted in increased tyrosine phosphorylation of endogenous PLC-γ1 (Fig. 6c). This result suggests that activated Syk sends signals to PLC-γ1 in hepatocytes, as observed in immune cells (Law *et al.*, 1996). Our findings that NS5A associates with Syk strongly suggest that NS5A affects the Syk signalosome to alter the signal transduction elicited by the Syk–PLC-γ1 interaction.

Phosphorylation of tyrosine residues in the linker region of Syk is required for immune receptor signalling. Genetic studies have demonstrated that phosphorylation of Tyr^{348} and Tyr^{352} in the linker region of Syk is involved in regulating tyrosine phosphorylation of LAT (linker for

activating T cells), SLP-76 and PLC-γ1 and -γ2, and affects Ca^{2+} mobilization triggered by aggregation of the high-affinity IgE receptor (Simon *et al.*, 2005; Zhang *et al.*, 2002). We observed that NS5A downregulated phosphorylation of Tyr^{352} of Syk (Fig. 6b), which correlated with the inhibition of Syk kinase activity. The phosphorylation state of Tyr^{352} also correlated well with the tyrosine phosphorylation state of PLC-γ1. This suggests the possibility that Ca^{2+} mobilization is affected in HCV-infected hepatocytes through the NS5A-mediated downregulation of Tyr^{352} phosphorylation on Syk.

Unlike ectopically expressed Syk, endogenously expressed Syk in B cells under normal conditions is not tyrosine phosphorylated (Wienands *et al.*, 1996). Pervanadate stimulation is known to induce tyrosine phosphorylation of endogenous Syk. We examined the possible interaction of endogenous Syk and NS5A. Our results demonstrated that NS5A interacted with endogenous Syk when the cells were treated with pervanadate, but not when the cells were left untreated (Fig. 2d). These results suggest that NS5A interacts with the tyrosine-phosphorylated, active form of Syk.

Whilst Syk is commonly expressed in normal human breast tissues, benign breast lesions and low-tumorigenic breast

−172−

cancer cell lines, only a minimal or even an undetectable level of Syk expression has been demonstrated in invasive breast carcinoma tissues and cell lines (Coopman *et al.*, 2000). DNA methylation of the CpG sites in the *syk* gene promoter has been reported to be responsible for the loss or marked reduction of Syk expression in breast cancer (Yuan *et al.*, 2001). Moreover, Yuan *et al.* (2006) reported that DNA methylation of the *syk* gene in hepatitis B virus-associated HCC cancerous tissue was highly correlated with Syk expression and that the patients with a methylated *syk* gene had a significantly lower overall survival rate after hepatectomy than those with an unmethylated *syk* gene. In contrast, our results revealed that the expression levels of Syk did not differ between normal and HCV-infected hepatocytes (Fig. 1k) or between cancerous and non-cancerous hepatocytes (data not shown). At the functional level, however, NS5A downregulated Syk kinase activity in Huh-7 cells (Fig. 6). Moreover, Syk kinase activity was downregulated in cells harbouring an HCV RNA replicon (Fig. 7c). These results collectively suggest that NS5A is involved, at least partly, in the suppression of Syk kinase activity in HCV-infected cells. It is also interesting to assume that the NS5A-mediated Syk inhibition plays an important role in the development of HCC, although the precise molecular mechanism(s) is yet to be determined. Recently, a possible mechanism by which breast cancer cells become invasive was proposed: human breast cancer cells express and secrete a group of chemokines called growth-related oncogene (GRO)-α, GRO-β and GRO-γ, and their production is regulated by Syk (Li & Sidell, 2005). It would be interesting to examine the possible effects of NS5A and HCV RNA replication on the levels of GRO expression and secretion.

ACKNOWLEDGEMENTS

REFERENCES

Blight, K. J., McKeating, J. A. & Rice, C. M. (2002). Highly permissive cell lines for subgenomic and genomic hepatitis C virus RNA replication. *J Virol* 76, 13001–13014.

Cheng, A. M., Rowley, B., Pao, W., Hayday, A., Bolen, J. B. & Pawson, T. (1995). Syk tyrosine kinase required for mouse viability and B-cell development. *Nature* 378, 303–306.

Choo, Q. L., Kuo, G., Weiner, A. J., Overby, L. R., Bradley, D. W. & Houghton, M. (1989). Isolation of a cDNA clone derived from a blood-borne non-A, non-B viral hepatitis genome. *Science* 244, 359–362.

Chung, K. M., Lee, J., Kim, J. E., Song, O. K., Cho, S., Lim, J., Seedorf, M., Hahm, B. & Jang, S. K. (2000). Nonstructural protein 5A of hepatitis C virus inhibits the function of karyopherin β3. *J Virol* 74, 5233–5241.

Coopman, P. J., Do, M. T., Barth, M., Bowden, E. T., Hayes, A. J., Basyuk, E., Blancato, J. K., Vezza, P. R., McLeskey, S. W. & other authors (2000). The Syk tyrosine kinase suppresses malignant growth of human breast cancer cells. *Nature* 406, 742–747.

Corey, S. J., Burkhardt, A. L., Bolen, J. B., Geahlen, R. L., Tkatch, L. S. & Tweardy, D. J. (1994). Granulocyte colony-stimulating factor receptor signaling involves the formation of a three-component complex with Lyn and Syk protein-tyrosine kinases. *Proc Natl Acad Sci U S A* 91, 4683–4687.

Costello, P. S., Turner, M., Walters, A. E., Cunningham, C. N., Bauer, P. H., Downward, J. & Tybulewicz, V. L. (1996). Critical role for the tyrosine kinase Syk in signalling through the high affinity IgE receptor of mast cells. *Oncogene* 13, 2595–2605.

Deng, L., Nagano-Fujii, M., Tanaka, M., Nomura-Takigawa, Y., Ikeda, M., Kato, N., Sada, K. & Hotta, H. (2006). NS3 protein of hepatitis C virus associates with the tumor suppressor p53 and inhibits its function in an NS3 sequence-dependent manner. *J Gen Virol* 87, 1703–1713.

Doi, H., Apichartpiyakul, C., Ohba, K. I., Mizokami, M. & Hotta, H. (1996). Hepatitis C virus (HCV) subtype prevalence in Chiang Mai, Thailand, and identification of novel subtypes of HCV major type 6. *J Clin Microbiol* 34, 569–574.

Evans, M. J., Rice, C. M. & Goff, S. P. (2004). Phosphorylation of hepatitis C virus nonstructural protein 5A modulates its protein interactions and viral RNA replication. *Proc Natl Acad Sci U S A* 101, 13038–13043.

Gale, M., Jr, Blakely, C. M., Kwieciszewski, B., Tan, S. L., Dossett, M., Tang, N. M., Korth, M. J., Polyak, S. J., Gretch, D. R. & Katze, M. G. (1998). Control of PKR protein kinase by hepatitis C virus nonstructural 5A protein: molecular mechanisms of kinase regulation. *Mol Cell Biol* 18, 5208–5218.

Gao, J., Zoller, K. E., Ginsberg, M. H., Brugge, J. S. & Shattil, S. J. (1997). Regulation of the pp72^{syk} protein tyrosine kinase by platelet integrin α$_{IIb}$β$_3$. *EMBO J* 16, 6414–6425.

Gao, L., Aizaki, H., He, J. W. & Lai, M. M. (2004). Interactions between viral nonstructural proteins and host protein hVAP-33 mediate the formation of hepatitis C virus RNA replication complex on lipid raft. *J Virol* 78, 3480–3488.

Ghosh, A. K., Majumder, M., Steele, R., Yaciuk, P., Chrivia, J., Ray, R. & Ray, R. B. (2000). Hepatitis C virus NS5A protein modulates transcription through a novel cellular transcription factor SRCAP. *J Biol Chem* 275, 7184–7188.

Goodman, P. A., Wood, C. M., Vassilev, A., Mao, C. & Uckun, F. M. (2001). Spleen tyrosine kinase (Syk) deficiency in childhood pro-B cell acute lymphoblastic leukemia. *Oncogene* 20, 3969–3978.

Hamamoto, I., Nishimura, Y., Okamoto, T., Aizaki, H., Liu, M., Mori, M., Abe, T., Suzuki, T., Lai, M. M. C. & other authors (2005). Human VAP-B is involved in hepatitis C virus replication through interaction with NS5A and NS5B. *J Virol* 79, 13473–13482.

He, Y., Nakao, H., Tan, S. L., Polyak, S. J., Neddermann, P., Vijaysri, S., Jacobs, B. L. & Katze, M. G. (2002). Subversion of cell signaling pathways by hepatitis C virus nonstructural 5A protein via interaction with Grb2 and P85 phosphatidylinositol 3-kinase. *J Virol* 76, 9207–9217.

Hidajat, R., Nagano-Fujii, M., Deng, L., Tanaka, M., Takigawa, Y., Kitazawa, S. & Hotta, H. (2005). Hepatitis C virus NS3 protein interacts with ELKS-δ and ELKS-α, members of a novel protein family involved in intracellular transport and secretory pathways. *J Gen Virol* 86, 2197–2208.

Kaneko, T., Tanji, Y., Satoh, S., Hijikata, M., Asabe, S., Kimura, K. & Shimotohno, K. (1994). Production of two phosphoproteins from the NS5A region of the hepatitis C viral genome. *Biochem Biophys Res Commun* 205, 320–326.

Kurosaki, T., Johnson, S. A., Pao, L., Sada, K., Yamamura, H. & Cambier, J. C. (1995). Role of the Syk autophosphorylation site and SH2 domains in B cell antigen receptor signaling. *J Exp Med* 182, 1815–1823.

Law, C. L., Chandran, K. A., Sidorenko, S. P. & Clark, E. A. (1996). Phospholipase C-γ1 interacts with conserved phosphotyrosyl residues in the linker region of Syk and is a substrate for Syk. *Mol Cell Biol* 16, 1305–1315.

Li, J. & Sidell, N. (2005). Growth-related oncogene produced in human breast cancer cells and regulated by Syk protein-tyrosine kinase. *Int J Cancer* 117, 14–20.

Lindenbach, B. D., Evans, M. J., Syder, A. J., Wolk, B., Tellinghuisen, T. L., Liu, C. C., Maruyama, T., Hynes, R. O., Burton, D. R. & other authors (2005). Complete replication of hepatitis C virus in cell culture. *Science* 309, 623–626.

Lohmann, V., Korner, F., Dobierzewska, A. & Bartenschlager, R. (2001). Mutations in hepatitis C virus RNAs conferring cell culture adaptation. *J Virol* 75, 1437–1449.

Macdonald, A. & Harris, M. (2004). Hepatitis C virus NS5A: tales of a promiscuous protein. *J Gen Virol* 85, 2485–2502.

Macdonald, A., Crowder, K., Street, A., McCormick, C. & Harris, M. (2004). The hepatitis C virus NS5A protein binds to members of the Src family of tyrosine kinases and regulates kinase activity. *J Gen Virol* 85, 721–729.

Maeda, N., Watanabe, M., Okamoto, S., Kanai, T., Yamada, T., Hata, J., Hozumi, N., Katsume, A., Nuriya, H. & other authors (2004). Hepatitis C virus infection in human liver tissue engrafted in mice with an infectious molecular clone. *Liver Int* 24, 259–267.

Majumder, M., Ghosh, A. K., Steele, R., Ray, R. & Ray, R. B. (2001). Hepatitis C virus NS5A physically associates with p53 and regulates p21/waf1 gene expression in a p53-dependent manner. *J Virol* 75, 1401–1407.

Mellor, J., Holmes, E. C., Jarvis, L. M., Yap, P. L. & Simmonds, P. (1995). Investigation of the pattern of hepatitis C virus sequence diversity in different geographical regions: implications for virus classification. *J Gen Virol* 76, 2493–2507.

Miah, S. M., Sada, K., Tuazon, P. T., Ling, J., Maeno, K., Kyo, S., Qu, X., Tohyama, Y., Traugh, J. A. & Yamamura, H. (2004). Activation of Syk protein tyrosine kinase in response to osmotic stress requires the interaction with p21-activated protein kinase Pak2/γ-PAK. *Mol Cell Biol* 24, 71–83.

Miyanari, Y., Atsuzawa, K., Usuda, N., Watashi, K., Hishiki, T., Zayas, M., Bartenschlager, R., Wakita, T., Hijikata, M. & Shimotohno, K. (2007). The lipid droplet is an important organelle for hepatitis C virus production. *Nat Cell Biol* 9, 1089–1097.

Muramatsu, S., Ishido, S., Fujita, T., Itoh, M. & Hotta, H. (1997). Nuclear localization of the NS3 protein of hepatitis C virus and factors affecting the localization. *J Virol* 71, 4954–4961.

Okamoto, K., Moriishi, K., Miyamura, T. & Matsuura, Y. (2004). Intramembrane proteolysis and endoplasmic reticulum retention of hepatitis C virus core protein. *J Virol* 78, 6370–6380.

Poole, A., Gibbins, J. M., Turner, M., van Vugt, M. J., van de Winkel, J. G., Saito, T., Tybulewicz, V. L. & Watson, S. P. (1997). The Fc receptor γ-chain and the tyrosine kinase Syk are essential for activation of mouse platelets by collagen. *EMBO J* 16, 2333–2341.

Qadri, I., Iwahashi, M. & Simon, F. (2002). Hepatitis C virus NS5A protein binds TBP and p53, inhibiting their DNA binding and p53 interactions with TBP and ERCC3. *Biochim Biophys Acta* 1592, 193–204.

Reed, K. E. & Rice, C. M. (2000). Overview of hepatitis C virus genome structure, polyprotein processing, and protein properties. *Curr Top Microbiol Immunol* 242, 55–84.

Robertson, B., Myers, G., Howard, C., Brettin, T., Bukh, J., Gaschen, B., Gojobori, T., Maertens, G., Mizokami, M. & other authors (1998). Classification, nomenclature, and database development for hepatitis C virus (HCV) and related virus: proposals for standardization. *Arch Virol* 143, 2493–2503.

Sada, K., Zhang, J. & Siraganian, R. P. (2000). Point mutation of a tyrosine in the linker region of Syk results in a gain of function. *J Immunol* 164, 338–344.

Sada, K., Takano, T., Yanagi, S. & Yamamura, H. (2001). Structure and function of Syk protein-tyrosine kinase. *J Biochem* 130, 177–186.

Schneider, F. & Kieser, A. (2004). A novel assay to quantify cell death after transient expression of apoptotic genes in B- and T-lymphocytes. *J Immunol Methods* 292, 165–174.

Shi, S. T., Polyak, S. J., Tu, H., Taylor, D. R., Gretch, D. R. & Lai, M. M. (2002). Hepatitis C virus NS5A colocalizes with the core protein on lipid droplets and interacts with apolipoproteins. *Virology* 292, 198–210.

Shiue, L., Green, J., Green, O. M., Karas, J. L., Morgenstern, J. P., Ram, M. K., Taylor, M. K., Zoller, M. J., Zydowsky, L. D. & other authors (1995). Interaction of p72^{syk} with the γ and β subunits of the high-affinity receptor for immunoglobulin E, FcεRI. *Mol Cell Biol* 15, 272–281.

Simon, M., Vanes, L., Geahlen, R. L. & Tybulewicz, V. L. (2005). Distinct roles for the linker region tyrosines of Syk in FcεRI signaling in primary mast cells. *J Biol Chem* 280, 4510–4517.

Song, J., Fujii, M., Wang, F., Itoh, M. & Hotta, H. (1999). The NS5A protein of hepatitis C virus partially inhibits the antiviral activity of interferon. *J Gen Virol* 80, 879–886.

Street, A., Macdonald, A., Crowder, K. & Harris, M. (2004). The hepatitis C virus NS5A protein activates a phosphoinositide 3-kinase-dependent survival signaling cascade. *J Biol Chem* 279, 12232–12241.

Taguchi, T., Nagano-Fujii, M., Akutsu, M., Kadoya, H., Ohgimoto, S., Ishido, S. & Hotta, H. (2004). Hepatitis C virus NS5A protein interacts with 2',5'-oligoadenylate synthetase and inhibits antiviral activity of IFN in an IFN sensitivity-determining region-independent manner. *J Gen Virol* 85, 959–969.

Takigawa, Y., Nagano-Fujii, M., Deng, L., Hidajat, R., Tanaka, M., Mizuta, H. & Hotta, H. (2004). Suppression of hepatitis C virus replicon by RNA interference directed against the NS3 and NS5B regions of the viral genome. *Microbiol Immunol* 48, 591–598.

Tan, S. L., Nakao, H., He, Y., Vijaysri, S., Neddermann, P., Jacobs, B. L., Mayer, B. J. & Katze, M. G. (1999). NS5A, a nonstructural protein of hepatitis C virus, binds growth factor receptor-bound protein 2 adaptor protein in a Src homology 3 domain/ligand-dependent manner and perturbs mitogenic signaling. *Proc Natl Acad Sci U S A* 96, 5533–5538.

Taniguchi, T., Kobayashi, T., Kondo, J., Takahashi, K., Nakamura, H., Suzuki, J., Nagai, K., Yamada, T., Nakamura, S. & Yamamura, H. (1991). Molecular cloning of a porcine gene *syk* that encodes a 72-kDa protein-tyrosine kinase showing high susceptibility to proteolysis. *J Biol Chem* 266, 15790–15796.

Tellinghuisen, T. L., Marcotrigiano, J. & Rice, C. M. (2005). Structure of the zinc-binding domain of an essential component of the hepatitis C virus replicase. *Nature* 435, 374–379.

Tsuchida, S., Yanagi, S., Inatome, R., Ding, J., Hermann, P., Tsujimura, T., Matsui, T. & Yamamura, H. (2000). Purification of a 72-kDa protein-tyrosine kinase from rat liver and its identification as Syk: involvement of Syk in signaling events of hepatocytes. *J Biochem* 127, 321–327.

Turner, M., Mee, P. J., Costello, P. S., Williams, O., Price, A. A., Duddy, L. P., Furlong, M. T., Geahlen, R. L. & Tybulewicz, V. L. (1995). Perinatal lethality and blocked B-cell development in mice lacking the tyrosine kinase Syk. *Nature* 378, 298–302.

Turner, M., Schweighoffer, E., Colucci, F., Di Santo, J. P. & Tybulewicz, V. L. (2000). Tyrosine kinase SYK: essential functions for immunoreceptor signalling. *Immunol Today* 21, 148–154.

Ulanova, M., Puttagunta, L., Marcet-Palacios, M., Duszyk, M., Steinhoff, U., Duta, F., Kim, M. K., Indik, Z. K., Schreiber, A. D. & Befus, A. D. (2005). Syk tyrosine kinase participates in β1-integrin signaling and inflammatory responses in airway epithelial cells. *Am J Physiol Lung Cell Mol Physiol* 288, L497–L507.

Wang, S., Ding, Y. B., Chen, G. Y., Xia, J. G. & Wu, Z. Y. (2004). Hypermethylation of Syk gene in promoter region associated with oncogenesis and metastasis of gastric carcinoma. *World J Gastroenterol* 10, 1815–1818.

Weiss, A. & Littman, D. R. (1994). Signal transduction by lymphocyte antigen receptors. *Cell* 76, 263–274.

Wienands, J., Larbolette, O. & Reth, M. (1996). Evidence for a preformed transducer complex organized by the B cell antigen receptor. *Proc Natl Acad Sci U S A* 93, 7865–7870.

Yamada, T., Fujieda, S., Yanagi, S., Yamamura, H., Inatome, R., Sunaga, H. & Saito, H. (2001). Protein-tyrosine kinase Syk expressed in human nasal fibroblasts and its effect on RANTES production. *J Immunol* 166, 538–543.

Yanagi, S., Kurosaki, T. & Yamamura, H. (1995). The structure and function of nonreceptor tyrosine kinase p72^{SYK} expressed in hematopoietic cells. *Cell Signal* 7, 185–193.

Yanagi, S., Inatome, R., Ding, J., Kitaguchi, H., Tybulewicz, V. L. & Yamamura, H. (2001). Syk expression in endothelial cells and their morphologic defects in embryonic Syk-deficient mice. *Blood* 98, 2869–2871.

Yasui, K., Wakita, T., Tsukiyama-Kohara, K., Funahashi, S. I., Ichikawa, M., Kajita, T., Moradpour, D., Wands, J. R. & Kohara, M. (1998). The native form and maturation process of hepatitis C virus core protein. *J Virol* 72, 6048–6055.

Yuan, Y., Mendez, R., Sahin, A. & Dai, J. L. (2001). Hypermethylation leads to silencing of the *SYK* gene in human breast cancer. *Cancer Res* 61, 5558–5561.

Yuan, Y., Wang, J., Li, M., Yan, Z., Zhang, C. & Dai, J. L. (2006). Frequent epigenetic inactivation of spleen tyrosine kinase gene in human hepatocellular carcinoma. *Clin Cancer Res* 12, 6687–6695.

Zech, B., Kurtenbach, A., Krieger, N., Strand, D., Blencke, S., Morbitzer, M., Salassidis, K., Cotten, M., Wissing, J. & other authors (2003). Identification and characterization of amphiphysin II as a novel cellular interaction partner of the hepatitis C virus NS5A protein. *J Gen Virol* 84, 555–560.

Zhang, J., Berenstein, E. & Siraganian, R. P. (2002). Phosphorylation of Tyr342 in the linker region of Syk is critical for Fc-εRI signaling in mast cells. *Mol Cell Biol* 22, 8144–8154.

Sequence Variation in Hepatitis C Virus Nonstructural Protein 5A Predicts Clinical Outcome of Pegylated Interferon/Ribavirin Combination Therapy

Ahmed El-Shamy,[1] Motoko Nagano-Fujii,[1] Noriko Sasase,[2] Susumu Imoto,[2] Soo-Ryang Kim,[2] and Hak Hotta[1,3]

A substantial proportion of hepatitis C virus (HCV)-1b–infected patients still do not re-
spond to interferon-based therapy. This study aims to explore a predictive marker for the
ultimate virological response of HCV-1b–infected patients treated with pegylated interfer-
on/ribavirin (PEG-IFN/RBV) combination therapy. Nonstructural protein 5A (NS5A) se-
quences of HCV in the pretreated sera of 45 patients infected with HCV-1b were analyzed.
The mean number of mutations in the variable region 3 (V3) plus its upstream flanking
region of NS5A (amino acid 2334-2379), referred to as IFN/RBV resistance-determining
region (IRRDR), was significantly higher for HCV isolates obtained from patients who later
achieved sustained virological response (SVR) by PEG-IFN/RBV than for those in patients
undergoing non-SVR. The receiver operating characteristic curve analysis estimated six
mutations in IRRDR as the optimal threshold for SVR prediction. Indeed, 16 (76%) of 21
SVR, but only 2 (8%) of 24 non-SVR, had HCV with six or more mutations in IRRDR
(IRRDR ≥ 6) ($P < 0.0001$). All of 18 patients infected with HCV of IRRDR of 6 or greater
examined showed a significant (≥1 log) reduction or disappearance of serum HCV core
antigen titers within 24 hours after initial dose of PEG-IFN/RBV, whereas 10 (37%) of 27
patients with HCV of IRRDR of 5 or less did ($P < 0.0001$). The positive predictive value of
IRRDR of 6 or greater for SVR was 89% (16/18; $P = 0.0007$), with its negative predictive
value for non-SVR being 81% (22/27; $P = 0.0008$). *Conclusion:* A high degree (≥6) of
sequence variation in IRRDR would be a useful marker for predicting SVR, whereas a less
diverse (≤5) IRRDR sequence predicts non-SVR. (HEPATOLOGY 2008;48:38-47.)

Hepatitis C virus (HCV) infection is the major
cause of chronic hepatitis, liver cirrhosis, and
hepatocellular carcinoma in industrialized
countries. However, HCV infection is curable, and its
complications can be prevented by antiviral therapy.[1,2]
Currently, the most effective treatment of chronic HCV
infection is based on a combination of pegylated inter-
feron (PEG-IFN) and ribavirin (RBV).[3] Even with this
treatment regimen, however, sustained virological re-
sponse (SVR) rates for those infected with the most resis-
tant genotypes, HCV-1a and HCV-1b, still hover at
approximately 50%.[3,4] Considering the high cost and the
significant side effects associated with this combination
therapy, it is worthy to identify patients most likely to
benefit from therapy.[5] Predictors of IFN-based therapy
can be classified into two categories, pretreatment and
on-treatment factors. Pretreatment factors comprise host
factors, such as age, sex, obesity, ethanol consumption,
hepatic iron overload, fibrosis, immune responses, and
coinfection with other viruses, and viral factors, which
mainly include viral genotypes and viral load. On-treat-
ment factors are mainly related to the viral kinetics within

the first few weeks of treatment.[6] Because the HCV genotype is one of the major factors affecting IFN-based therapy response, IFN resistance is, at least partly, genetically encoded by HCV itself.[7] In this context, nonstructural protein 5A (NS5A), one of the HCV nonstructural proteins, has been widely discussed for its correlation with IFN responsiveness. Enomoto et al.[8,9] proposed that the sequence variations within a region in NS5A, called the IFN sensitivity-determining region (ISDR), is correlated with IFN responsiveness. It was further demonstrated that ISDR and its adjacent sequence was able to bind to double-stranded RNA-activated protein kinase (PKR), one of the important antiviral proteins of the host cell, to inhibit its enzymatic activity and, therefore, the combined region is called PKR-binding domain (PKR-BD).[10,11] A significant correlation between sequence variation in PKR-BD and IFN responsiveness was also reported.[12] In addition, there are some reports that showed a correlation between IFN responsiveness and the sequence diversity of the variable region 3 (V3) [amino acids (aa) 2356 to 2379] or its surrounding regions near the carboxy terminus of NS5A.[12-20]

We have recently reported that a high degree of sequence variations in the V3 and the pre-V3 regions (aa 2334-2355) of NS5A, which we collectively refer to as IFN/RBV resistance-determining region (IRRDR) (aa 2334-2379), was closely correlated with early virological response (EVR) by week 16 in HCV-1b–infected patients treated with PEG-IFN and RBV.[21] In the current study, we aimed to follow up our previous observations to investigate whether the degree of sequence variation in IRRDR could also correlate with SVR on PEG-IFN/RBV combination therapy.

Patients and Methods

Patients. A total of 45 patients chronically infected with HCV-1b, whose diagnoses had been made based on anti-HCV antibody detection, HCV subtype determination according to the method by Okamoto et al.,[22] and clinical follow-up, were treated with PEG-IFN α-2b (1.5 μg/kg body weight, once weekly, subcutaneously) and RBV (600-800 mg daily, per os), according to a standard treatment protocol for Japanese patients established by a hepatitis study group of the Ministry of Health, Labour, and Welfare, Japan, at Kobe Asahi Hospital, Hyogo Prefecture, Japan. All the patients were confirmed negative for hepatitis B surface antigen using chemiluminescent immunoassay (Abbott Japan Co., Ltd., Tokyo, Japan). Serum samples were collected from the patients at intervals of 4 weeks before, during, and after the treatment, and tested for HCV RNA by reverse transcription poly-

merase chain reaction (RT-PCR), as reported previously.[21] The quantification of serum HCV RNA titers was performed by RT-PCR with an internal RNA standard derived from the 5' noncoding region of HCV (Amplicor HCV Monitor test, version 2.0, Roche Diagnostics, Tokyo, Japan). The thresholds of the low-range and high-range measurements of this assay were 50 and 600 IU/mL, respectively. HCV core antigen in the sera was also quantitatively measured by chemiluminescent immunoassay (Abbott Japan Co., Ltd., Tokyo, Japan). The threshold of this assay is 20 fmol/L.

The study protocol was approved beforehand by the Ethic Committee in Kobe Asahi Hospital, and written informed consent was obtained from each patient before the treatment.

NS5A Sequence Analysis. HCV RNA was extracted from 140 μL serum using a commercially available kit (QIAmp viral RNA kit; QIAGEN, Tokyo, Japan). For amplification of the NS5A region of the HCV genome, the extracted RNA was reverse transcribed and amplified for full-length NS5A using SuperScript One-step RT-PCR for long templates (Invitrogen, Tokyo, Japan) and a set of primers, NS5A-F1 [5'-TACTCCCTGCCATC-CTCTCTCCTG-3'; sense, nucleotides (nt) 5974-5997] and NS5A-F2 (5'-CTCCTTGAGCACGTCCCGGT-3'; antisense, nt 7777-7796). The resultant RT-PCR product was subjected to a second-round PCR by using Platinum Taq DNA polymerase (Invitrogen) and an inner set of primers, NS5A-F3 (5'TCTCCAGCCTTAC-CATCACYCA-3'; sense, nt 6172-6193) and NS5A-F4 (5'-CGGTARTGRTCGTCCAGGAC-3'; antisense, nt 7761-7780). The samples that were not amplifiable (nos. 3, 23, 47, 61, 65, and 69) using the aforementioned primers were amplified using primer sets reported previously.[23] Reverse transcription was performed at 45°C for 30 minutes and terminated at 94°C for 2 minutes, followed by the first-round PCR over 35 cycles, with each cycle consisting of denaturation at 94°C for 30 seconds, annealing at 55°C for 30 seconds and extension at 68°C for 90 seconds. The second-round PCR was performed under the same condition. The amplified fragments were purified with QIA quick PCR purification kit (QIAGEN), and visualized by agarose gel electrophoresis and ethidium bromide staining. The sequences of the amplified fragments were determined by direct sequencing without subcloning using Big Dye Deoxy Terminator cycle sequencing kit and ABI 337 DNA sequencer (Applied Biosystems, Inc, Japan). The aa sequences were deduced and aligned using GENETYX Win software version.7.0 (GENETYX Corp., Tokyo, Japan). Numbering of aa throughout the complete manuscript is according to the poly protein of HCV genotype 1b prototype HCV-J.[24]

Statistical Analysis. Statistical difference in the parameters, including all available patients' demographic, biochemical, hematological, and virological data as well as IRRDR sequence variations factors, was determined between different patients' groups by Student *t* test for numerical variables, and Fisher's exact probability test for categorical variables. In the case of multiple comparisons for various regions of NS5A, *P* values were adjusted by the Bonferroni method to reduce the probability of erroneously classifying nonsignificant hypothesis as significant. Although there are five regions of comparison (full-NS5A, N-half, ISDR, PKR-BD and IRRDR), the ISDR is entirely within the PKR-BD, and all the regions fall within the full-NS5A. Therefore, it would be reasonable to adjust the *P* values for three regions of comparison. Accordingly, the *P* value for a test was multiplied by 3. To evaluate the optimal threshold of IRRDR mutations for SVR prediction, the receiver operating characteristic curve was constructed and the area under the curve as well as the sensitivity and specificity were calculated. Subsequently, univariate and multivariate logistic analyses were performed to identify variables that independently predict SVR. The odds ratios and 95% confidence intervals (95% CI) were also calculated. Kaplan-Meier HCV survival curve analysis was performed based on serum HCV-RNA positivity data during treatment period (48 weeks) according to the number of IRRDR mutations (IRRDR $\geq$ 6 and IRRDR $\leq$ 5). The HCV death event was estimated as the first time point of HCV-RNA clearance after initiation of the treatment. The data obtained were evaluated by the log-rank test. Positive and negative predictive values of SVR predictors were computed, and their significance levels were evaluated using the sign test. All statistical analyses were performed using the SPSS version 16 software (SPSS Inc., Chicago, IL). Unless otherwise stated, a *P* value of less than 0.05 was considered statistically significant.

Nucleotide Sequence Accession Numbers. The sequence data reported in this article have been deposited in the DDBJ/EMBL/GenBank nucleotide sequence databases with the accession numbers AB285035 through AB285081, and AB354116 through AB354118.

Results

Virological Responses of the Patients Treated with PEG-IFN and RBV. Proportions of various virological responses of the patients treated with PEG-IFN/RBV combination therapy are shown in Table 1. Of 45 patients enrolled in this study, 23 (51%), 31 (69%), and 21 (47%) patients, respectively, achieved EVR by week 12 [EVR(12w)], end-of-treatment response (ETR), and sus-

Table 1. Proportions of Various Virological Responses of Patients Treated With PEG-IFN/RBV

Virological Response	Proportion
EVR(12w)	51% (23/45)*
ETR	69% (31/45)
SVR	47% (21/45)
Non-SVR	53% (24/45)
CNR	24% (11/45)
Relapse	29% (13/45)
ETR-relapse	22% (10/45)
Viral breakthrough	7% (3/45)

*No. of patients/no. of total.
Abbreviations: PEG-IFN/RBV, pegylated-interferon/ribavirin; EVR, early virological response; ETR, end-of-treatment response; SVR, sustained virological response; CNR, complete nonresponse.

tained virological response (SVR). Among 23 patients with EVR(12w), 22 (96%) and 18 patients (78%) achieved ETR and SVR, respectively. This indicates that EVR(12w) was significantly correlated with ETR and SVR ($P < 0.0001$). A total of 24 patients (53%) failed to achieve SVR, and they were referred to as non-SVR. Non-SVR can be divided into two categories: (i) complete nonresponse (CNR), which is defined by continued presence of serum HCV RNA up to the end of the treatment, and (ii) relapse, which is defined by transient disappearance of HCV RNA at a certain time point followed by reappearance of HCV RNA either before or after the end of the treatment. CNR represented 24% (11/45) of all cases and 46% (11/24) of non-SVR. Thirteen (29%) of 45 patients underwent relapse. Among 13 relapsers, 3 (23%) patients had rebound in HCV viremia before the end of the treatment and, hence, were defined as undergoing viral breakthrough, whereas 10 (77%) patients had rebound in HCV viremia after the end of the treatment, defined as ETR-relapsers.

Demographic characteristics of patients with SVR, non-SVR, CNR, and relapse are summarized in Table 2. Age, sex, body weight, hemoglobin levels, or gamma guanosine triphosphate titers did not significantly differ between SVR and non-SVR or CNR. However, patients with SVR showed a trend toward having significantly higher platelet counts than those with non-SVR and CNR. Also, the mean initial titers of HCV core antigen for non-SVR and CNR, respectively, were 1.6 times and 2.3 times higher than that for SVR, although the difference was not statistically significant. HCV RNA titers were almost the same among them.

Correlation Between Virological Responses and the Sequence Variation of IRRDR of HCV NS5A Obtained from the Pretreated Sera. The entire NS5A region of the HCV genome was amplified from the pretreated sera and the aa sequences deduced. We compared

Table 2. Demographic Characteristics of Patients With SVR, Non-SVR, CNR, and Relapse

Factor	SVR	Non-SVR	CNR	Relapse	SVR versus Non-SVR	SVR versus CNR	SVR versus Relapse
					P Value		
Age	56.5 ± 8.0*	59.9 ± 10.6	59.4 ± 10.0	60.3 ± 11.5	NS†	NS	NS
Sex (male/female)	12/9	13/11	6/5	7/6	NS	NS	NS
Body weight (kg)	58.5 ± 9.4	59 ± 13.2	61.0 ± 10.8	57.8 ± 15.3	NS	NS	NS
Platelets ($\times 10^4/mm^3$)	18.3 ± 4.4	15.0 ± 4.9	12.3 ± 3.9	16.8 ± 4.9	0.02‡	0.001‡	NS
Hemoglobin (g/dL)	14.1 ± 1.3	13.7 ± 1.4	14.4 ± 1.3	14.3 ± 1.5	NS	NS	NS
γ-GTP (IU/L)	43.5 ± 28.7	51.6 ± 35.7	62.8 ± 40.3	43.8 ± 30.5	NS	NS	NS
HCV-RNA (KIU/mL)	1326 ± 1256	1667 ± 1311	1488 ± 1228	1818 ± 1408	NS	NS	NS
HCV core antigen (fmol/L)	6183 ± 6894	9830 ± 1214	14,033 ± 17,089	6481 ± 4023	NS	NS	NS

*Mean ± SD.
†Not significant.
‡Student *t* test.
Abbreviations: SVR, sustained virological response; CNR, complete nonresponse; γ-GTP, gamma guanosine triphosphate.

each NS5A sequence with a consensus sequence inferred from aligning the previously published NS5A-1b sequences.[8] In this connection, the consensus sequence for IRRDR differs from the corresponding sequence of a prototype strain of IFN resistance HCV-1b (HCV-J; DDBJ/EMBL/Genbank accession no. D90208) by a single residue at position 2367 (Ala instead of Gly). Because Ala[2367] was conserved in 95% of the reported sequences, we used the IRRDR consensus sequence in this study. As shown in Table 3, the mean number of aa substitutions in the entire NS5A obtained from patients with SVR was significantly greater compared with non-SVR and relapse. There was no difference in the number of mutations in an N-terminal half of NS5A (aa 1972-2208), the ISDR (aa 2209-2248) or the PKR-BD (aa 2209-2274) between different patients' groups. Conversely, we found a more obvious significant difference in the mean numbers of aa mutations within a region consisting of the pre-V3 and V3 regions, which we refer to as IRRDR, between SVR and other patients' groups (Table 3).

To estimate a cutoff number of mutations in IRRDR predicting SVR, the receiver operating characteristics analysis was performed. The result revealed that six mutations were an optimal number of mutations to predict SVR, because it achieved the highest sensitivity (76%) combined with the highest specificity (92%) and yielded an area under the curve of 0.81 (Fig. 1).

Indeed, only 2 (8%) of 24 patients with non-SVR, in contrast to 16 (76%) of 21 patients with SVR, had HCV with IRRDR of 6 or greater, with the difference between the two groups being statistically significant ($P < 0.0001$) (Table 4). Furthermore, none of 11 patients with CNR had HCV of IRRDR of 6 or greater, and the difference between SVR and CNR was statistically significant ($P < 0.0001$). Similarly, only 2 (15%) of 13 relapsers (10 ETR-relapsers + 3 patients with viral breakthrough) had HCV of IRRDR greater than or equal to 6, with the result demonstrating significant difference between SVR and relapse ($P = 0.001$).

Table 3. Average Numbers of aa Mutations Within Different Regions of HCV NS5A Obtained From Pretreated Sera of Patients With SVR, Non-SVR, CNR, and Relapse

NS5A Region	SVR	Non-SVR	CNR	Relapse	SVR versus Non-SVR	SVR versus CNR	SVR versus Relapse
	No. of Mutations*				*P* Value†		
Full-NS5A (aa 1972-2419)	24.9 ± 6.1*	19.7 ± 4.3	20.1 ± 5.2	19.4 ± 3.5	0.012	0.144	0.03
N-half (aa 1972-2208)	9.2 ± 1.9	8.6 ± 1.9	9.0 ± 2.4	8.2 ± 1.2	NS‡	NS	NS
ISDR (aa 2209-2248)	2.1 ± 2.8	1.2 ± 1.1	1.7 ± 1.4	0.8 ± 0.7	NS	NS	NS
PKR-BD (aa 2209-2274)	3.8 ± 3.4	2.5 ± 2.0	2.9 ± 2.4	2.1 ± 1.5	NS	NS	NS
IRRDR (aa 2334-2379)	6.1 ± 2.1	3.9 ± 1.4	3.7 ± 0.9	4.0 ± 1.8	0.0006	0.003	0.018

*Mean ± SD.
†The *P* values obtained with Student *t* test were adjusted using the Bonferroni method (see Materials and Methods).
‡Not significant.
Abbreviations: SVR, sustained virological response; CNR, complete nonresponse; aa, amino acid; ISDR: interferon sensitivity-determining region; PKR-BD, double-stranded RNA-activated protein kinase-binding domain; IRRDR, interferon/ribavirin resistance-determining region.
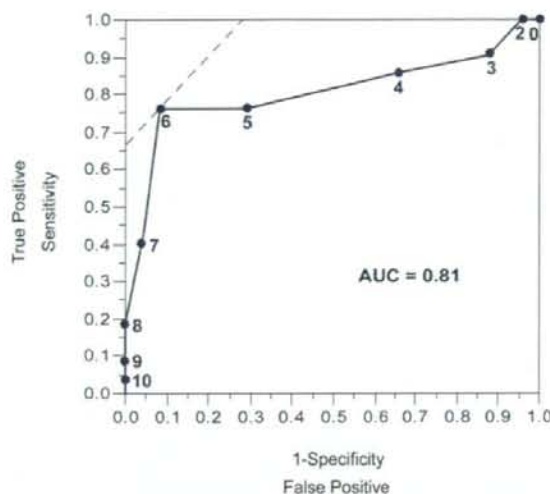
Fig. 1. The receiver operating characteristic curve analysis of IRRDR sequence variation for SVR prediction. The curve depicted with solid line shows an area under the curve of 0.81. Solid circles with numerals plotted on the curve represent different numbers of IRRDR mutations analyzed. The dashed line in the upper left corner indicates the optimal number of IRRDR mutations for SVR prediction, which yields the highest sensitivity (76%) and the highest specificity (92%).

When the IRRDR sequences obtained from all 45 patients were aligned along with the consensus sequence (Fig. 2), we noticed that 10 (48%) of 21 patients with SVR had alanine at position 2360 (Ala^{2360}), whereas only 3 (13%) of 24 patients with non-SVR and none of 11 patients with CNR did ($P = 0.02$ and 0.006, respectively) (Table 4). Similarly, 9 (43%) of 21 patients with SVR had threonine at position 2378 (Thr^{2378}), whereas only 3 (13%) of 24 patients with non-SVR and none of 11 patients with CNR did ($P = 0.04$ and 0.01, respectively).

To identify significant independent SVR predictors, we first entered all available baseline patients' features and IRRDR sequence variations data in univariate logistic analysis. As had been expected, this analysis yielded four factors significantly associated with SVR: IRRDR muta-

tions, either continuous variable ($P < 0.0001$) or dichotomized at 6 ($P < 0.0001$), Ala^{2360} ($P = 0.002$), Thr^{2378} ($P = 0.019$), and platelet count ($P = 0.017$). Subsequently, we analyzed these four factors by multivariate logistic analysis. When the IRRDR mutations were dichotomized at 6, the multivariate analysis identified only the IRRDR of 6 or greater criterion as the independent predictor of SVR (odds ratio = 16.0; CI, 2.4-104.3; $P = 0.004$) (Table 5). However, when the IRRDR mutations were analyzed as a continuous variable, the multivariate analysis yielded IRRDR mutations (odds ratio = 1.8; CI, 1.1-3.1; $P = 0.02$) and Ala^{2360} (odds ratio = 9.3; CI, 1.1-78.8; $P = 0.04$) as independent SVR predictors.

Figure 3A shows the viral clearance rates of patients infected with HCV of IRRDR of 6 or greater and those with IRRDR of 5 or less at 4-week intervals during the whole observation period (72 weeks). All of 18 patients infected with HCV of IRRDR 6 or greater cleared the virus by week 16 and remained free of viremia thereafter until the end of the PEG-IFN/RBV treatment (week 48). Within 4 weeks after the cessation of the combination therapy, however, 2 (11%) of the 18 patients underwent relapse (ETR relapse). Conversely, 16 (59%) of the 27 patients with HCV of IRRDR of 5 or less cleared the virus by week 32. Of the 16 patients who once cleared the virus, 3 (19%) and 8 (50%) underwent relapse to become viral breakthrough and ETR relapsers, respectively.

Kaplan-Meier HCV survival curve analysis confirmed that, after the initiation of the IFN/RBV treatment, HCV clearance was achieved significantly more rapidly in patients infected with HCV isolates with IRRDR of 6 or greater than those with IRRDR of 5 or less, with the difference between the two groups being statistically significant ($P < 0.0001$) (Fig. 3B).

Sequence Analysis of ISDR and PKR-BD of HCV NS5A Obtained from Pretreated Sera. As described, there was no difference in the mean number of mutations in ISDR or PKR-BD between SVR and non-SVR or CNR (Table 3). Only four patients had HCV with four or

Table 4. Correlation Between NS5A Sequence Variation and Virological Responses of the Patients

	No. of Subjects / no. of Total*				P Value†		
Criteria	SVR	Non-SVR	CNR	Relapse	SVR versus Non-SVR	SVR versus CNR	SVR versus Relapse
IRRDR ≥ 6	16/21 (76%)	2/24 (8%)	0/11 (0%)	2/13 (15%)	< 0.0001	< 0.0001	0.001
Ala^{2360}	10/21 (48%)	3/24 (13%)	0/11 (0%)	3/13 (23%)	0.02	0.006	NS‡
Thr^{2378}	9/21 (43%)	3/24 (13%)	0/11 (0%)	3/13 (23%)	0.04	0.01	NS

*Total no. of SVR, Non-SVR, CNR, or relapse.
†Fisher's exact test.
‡Not significant.
Abbreviations: SVR, sustained virological response; CNR, complete nonresponse; IRRDR, interferon/ribavirin resistance-determining region; Ala^{2360}, alanine at position 2360; Thr^{2378}, threonine at position 2378.